



Università degli Studi di Napoli Federico II

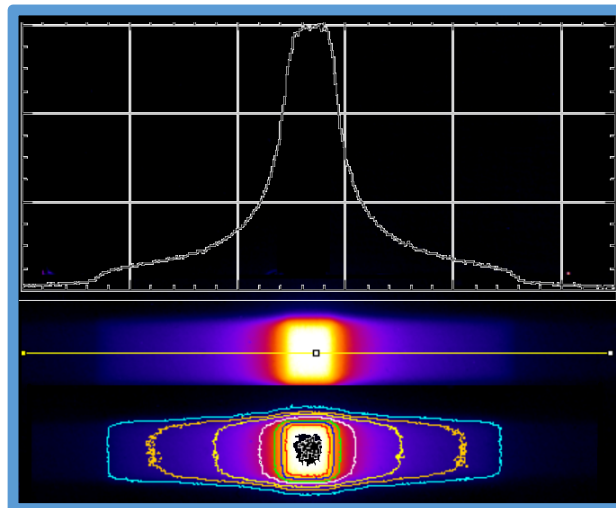
Scuola Politecnica e delle Scienze di Base
Collegio di Scienze

Dipartimento di Fisica “Ettore Pancini”

Corso di Laurea Magistrale in Fisica

TESI DI LAUREA SPERIMENTALE IN FISICA MEDICA

***Synchrotron radiation rotational radiotherapy:
a new technique for breast cancer treatment***



Relatore

Prof. Paolo Russo

Candidata

Dott.ssa Marica Masi
matr. N94000382

Anno Accademico 2016/2017

Università degli Studi di Napoli Federico II



*Synchrotron radiation rotational radiotherapy:
a new technique for breast cancer treatment*

by

Marica Masi (B.Sc. Physics, 2016)

This thesis work was carried out during August 2017 - March 2018, in partial fulfilment of the requirements for the Diploma di Laurea Magistrale in Fisica (M.Sc. Physics) at University of Naples "Federico II", Naples, Italy

The Istituto Nazionale di Fisica Nucleare (INFN) (Italy) approved scientifically and funded the research activities carried out in this work, within the research project SR³T.

The following Institutions kindly provided access to their research or hospital facilities for the purposes of this work:



Istituto Nazionale di Fisica Nucleare, Sezione di Napoli, Naples, Italy



Ospedale San Raffaele, Milan, Italy

*Non si ottiene sempre ciò che si desidera,
si ottiene ciò per cui si lavora.*

List of contents

Index of abbreviations	1
Introduction	2
Chapter 1 Radiotherapy of breast cancer	4
1.1 Whole Breast Irradiation (WBI)	4
1.1.1 Definition of terms	6
1.1.2 Direct planning: 3D-CRT	8
1.1.3 Inverse planning: VMAT	10
1.2 Partial breast Irradiation (PBI)	13
1.3 Accelerated Partial Breast Irradiation (APBI)	13
1.4 Stereotactic Partial Breast Irradiation (S-PBI)	14
1.5 Kilovoltage Rotational Radiotherapy with X-ray tube (kV-EBRT)	15
1.6 Synchrotron Radiation Rotational Radiotherapy for breast cancer (SR ³ T)	17
Chapter 2 Experimental validation of the SR³T technique	19
2.1 Dose distribution in breast phantom at 100 keV with synchrotron radiation	19
2.1.1 Radiochromic film dosimetry at 100 keV	19
2.1.2 Measurements in breast phantom at 100 keV	23
2.2 Dose distribution in breast phantom at 6 MV in VMAT	27
2.2.1 Radiochromic film dosimetry at 6 MV	27
2.2.2 Eclipse TM TPS for phantom irradiation	28
2.2.3 Measurements at San Raffaele Hospital	30
Conclusions	46
Bibliography	47
Acknowledgements	49

Index of abbreviations

Abbreviation	Explanation
3D-CRT	three-Dimensional Conformal Radiotherapy
APBI	Accelerated Partial Breast Irradiation
bCT	dedicated breast Computed Tomography
BEV	Beam's Eye of View
CT	Computed Tomography
CTV	Clinical Target Volume
DVH	Dose Volume Histogram
EBRT	External Beam Radiotherapy
EBT	External Beam Therapy
GTV	Gross Tumour Volume
ICRU	International Commission on Radiation Units and measurements
IMBL	Imaging and Medical Beamline
IMRT	Intensity Modulated Radiation Therapy
IORT	Intra Operative Radiation Therapy
ITV	Internal Target Volume
kV-EBRT	Kilovoltage External Beam Rotational Radiotherapy
LINAC	Lineal Accelerator
MRI	Magnetic Resonance Imaging
OD	Optical Density
PBI	Partial Breast Irradiation
PTV	Planning Target Volume
PV	Pixel Value
QA	Quality Assurance
ROI	Region Of Interest
RT	Radiotherapy
RTOG	Radiation Therapy Oncology Group
S-PBI	Stereotactic Partial Breast Irradiation
S-BRT	Stereotactic Body Radiation Therapy
SAD	Source-to-Axis Distance
SR	Synchrotron Radiation
SR ³ T	Synchrotron Radiation Rotational Radiotherapy
SSD	Source-to-Surface Distance
SYRMEP	SYnchrotron Radiation for MEDical Physics
TIFF	Target File Format
TPS	Treatment Planning System
VMAT	Volumetric Modulated Arc Therapy
WBI	Whole Breast Irradiation

Introduction

Breast cancer is the most common cancer in women. The standard care requires an early diagnosis by mammography screening, tumour mass surgery, chemotherapy and radiotherapy (RT) to sterilize the breast area. The conventional technique for breast radiotherapy is megavoltage photon three-dimensional conformal radiotherapy (3D-CRT) with X-ray beams, using a medical linear accelerator (LINAC), but in last years also other techniques are under investigation. Research in breast cancer therapy includes the use of limited number of fraction in order to reduce the treatment time and the search for irradiation strategies in order to decrease the dose to normal organs such as the heart, the carotid arteries and the lungs, and the contralateral breast.

Research is also active for breast cancer 3D imaging, and the National Institute of Nuclear Physics (INFN) in Italy (National Scientific Commission no. 5 for research in technological, interdisciplinary and accelerator physics) started a project for breast computed tomography with synchrotron radiation: the medical physics group in Napoli is involved in the dosimetric aspects. Within this activity, the Napoli group proposed the SR³T (*Synchrotron Radiation Rotational Radiotherapy*) project for breast radiotherapy using a synchrotron radiation source. Indeed, the same high flux beam can be used for imaging and for cancer radiotherapy. In this geometry the horizontal beam irradiates the breast hanging from a hole in the patient bed. Rotation and translation of the bed permits to irradiate the breast over 360 degrees, so implementing a new technique for rotational breast radiotherapy. In this project, rotation of the low energy beam around the breast permits to accumulate the dose along the axis of rotation, so realizing a tumour-to-skin dose ratio similar to that of conventional breast radiotherapy with 6 MV beam.

While extensive tests have been performed at ESRF (France) and AS (Australia) synchrotrons with breast phantoms irradiated at 60-175 keV monoenergetic beams, no comparison was available for showing the differences in volume distribution between kilovoltage and megavoltage photon beams in the propose SR³T technique.

This thesis is dedicated to answer this investigative goal, via irradiation carried out with a clinical accelerator and the same breast phantom adopted in the synchrotron irradiations. The thesis is divided in two chapters. First chapter is focused on conventional radiotherapy techniques for breast cancer and on new techniques for rotational radiotherapy with an

orthovoltage X-ray tube and with synchrotron radiation (the SR³T project). In the second chapter, after summarising the results of the previous work carried out at Imaging and Medical Beamline (IMBL) of Australian Synchrotron (AS) (Melbourne, Australia), my work carried out at San Raffaele Hospital in Milan, Italy, with a clinical linac is described.

Chapter 1

Radiotherapy of breast cancer

1.1 Whole Breast Irradiation (WBI)

Breast cancer affects one in eight women over a lifetime. It is the most common cancer in women and accounts for 29% of all cancers affecting women. It is the first cause of cancer mortality in women, with a mortality rate of 17% of all deaths due to cancer on women [1]. In case of breast cancer the standard therapeutic procedure involves tumour mass surgery first and then chemotherapy and postoperative radiotherapy (RT) to sterilize the breast area (to remove any cancer cell that may be left) and reduce the risk of recurrences. For this reason conventional radiotherapy involves whole breast irradiation (WBI). The commonly used technique for WBI is megavoltage photon three-dimensional conformal radiotherapy (3D-CRT) with x-ray beams, using a medical linear accelerator (LINAC). 3D-CRT is based on 3D anatomic information (provided e.g. by computed tomography or magnetic resonance imaging scans) and uses tangential fields that conform as closely as possible to the target volume in order to deliver adequate dose to the tumour and minimum possible dose to normal tissues [2]. In this conventional RT technique the woman is in a supine position on the treatment couch (Fig. 1.1).



Figure 1.1: Conventional breast radiotherapy with a linac (from: <http://radonc.radiationnation.com>)

Before starting the radiotherapy, the patient is required to do a diagnostic computed tomography (CT) scan to identify the exact target tissue position. To identify the isocentre of the irradiation field and to reduce troubles due to the patient repositioning, metallic marks, called “reperi”, with high atomic number, are placed on the patient after CT scan. At this

point the radiation oncologist contours the organs' shape, and gives the dose prescription. The gold standard of dose prescription is 50 Gy in 25 fractions of 2 Gy per fraction (but the protocol at San Raffaele Hospital used for reference in this work consists of 40 Gy in 15 fractions of 2.667 Gy per fraction). Then, medical physicists use the treatment-planning software (TPS) to design fields and beam arrangements, and carries out the corresponding quality assurance (QA) tests. The effectiveness of the breast radiotherapy strongly depends on the radiation dosimetry: the 3D treatment planning system application is essential in order to provide an accurate dose model taking into due consideration also the scattered radiation. In addition, conventional radiotherapy allows skin sparing and avoids skin tissue complications after RT, making use of a 6-MV X-ray beam which produces the build-up effect and so reduces the dose to the skin to a fraction of the maximum dose at depth in the tissue [3].

On the other hand, one of the critical issue of breast radiotherapy is the associated increased rate of ischemic heart disease, especially in patients treated for left-sided breast cancer [4]: with improved survival rates, it was observed that a higher number of patients will be at risk in the long-term. As the rate of the ischemic heart disease is proportional to the mean heart dose, the goal is to reduce the dose to the heart as much as possible. Hence the Intensity Modulated Radiotherapy (IMRT) with photons has been investigated to improve the dose homogeneity and to additionally reduce the doses to surrounding organs at risk. Then, 3D TPS, deep inspiration breath-hold, and prone position, instead of supine position, are implemented to minimize cardiopulmonary dose for patients. [5].

Another inconvenient of WBI is that it requires from 3 to 6.5 weeks of daily treatments [6]. This can make completing a course of radiotherapy difficult for elderly, financially strained patients, patients with transportation difficulty, or patients who live far from a radiation facility. This discomfort can involve health disparities in some patients and can lead to not completing breast radiotherapy. Shortening the overall time of breast irradiation treatments may lessen the disparity gap and improve treatment compliance [6].

Conventional radiotherapy includes the following techniques:

- Direct planning, that is the 3D-CRT;
- Inverse planning, that is the Volumetric Modulated Arc Therapy (VMAT).

1.1.1 Definition of terms

Volume definition is an important prerequisite for 3D treatment planning, so ICRU (International Commission on Radiation Units and Measurements), Reports No. 50 and 62, define the following principal volumes [7] (Fig. 1.2):

- *Gross tumour volume*

“The Gross Tumour Volume (GTV) is the gross palpable or visible/demonstrable extent and location of malignant growth” (ICRU Report No. 50). The GTV is obtained from CT, magnetic resonance imaging (MRI), ultrasound, histological reports and clinical examinations.

- *Clinical target volume*

“The clinical target volume (CTV) is the tissue volume that contains a demonstrable GTV and/or sub-clinical microscopic malignant disease, which has to be eliminated. This volume thus has to be treated adequately in order to achieve the aim of therapy, cure or palliation” (ICRU Report No. 50). The CTV includes the area surrounding the GTV which may contain microscopic disease and other areas considered at risk. It is an anatomical-clinical volume and is determined by the radiation oncologist.

- *Internal target volume*

The internal target volume (ITV) consists of the CTV plus a margin. It is designed to take into account the variation in the size and position of the CTV due to organ motion such as breathing and bladder or rectal contents (ICRU Report No. 62). Patient motion can give rise to systematic as well as random errors that must be accounted for when designing the ITV.

- *Planning target volume*

“The planning target volume (PTV) is a geometrical concept, and it is defined to select appropriate beam arrangements, taking into consideration the net effect of all possible geometrical variations, in order to ensure that the prescribed dose is actually absorbed in the CTV” (ICRU Report No. 50). The PTV includes the ITV and an additional margin for set-up uncertainties, machine tolerances and intra-treatment variations. The PTV depends on the precision of tools as immobilization devices and lasers, but does not include a margin for the dosimetric characteristics of the radiation beam (i.e. penumbral areas and build-up region), as these will require an additional margin during treatment planning.

- *Organ at risk*

The organ at risk is an organ whose sensitivity to radiation is such that the dose received from a treatment plan may be significant compared with its tolerance.

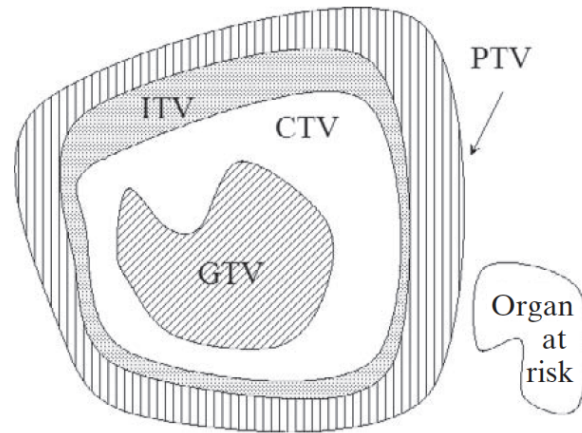


Figure 1.2: Graphical representation of the volumes of interest, as defined in ICRU Reports No. 50 and 62.

ICRU Report No. 23 and 50 define several dosimetric end points: minimum target dose, maximum target dose and mean target dose. The ICRU reference point dose is located at a point chosen to represent the delivered dose using the following criteria:

- the point should be located in a region where the dose can be calculated accurately (i.e. no build-up or steep gradient);
- the point should be in the central part of the PTV;
- the isocentre is recommended as ICRU reference point.

A 3D treatment plan consists of dose distribution values over a 3D matrix of points over the patient's anatomy, called Dose-Volume Histogram (DVH). DVHs summarize the information contained in the 3D dose distribution and are powerful tools for quantitative evaluation of treatment plans. A DVH represents 'per cent volume of total volume' on the ordinate against the dose on the abscissa. The ideal DVH for the PTV would be a single column indicating that 100% of the volume receives 100% of the prescribed dose although the minimum acceptable requirement is that the 95% of the PTV receives the 95% of the dose. The reason why the ideal DVH is not achievable is the presence of surrounding organs at risk to be saved. Actually, also to ensure that 100% of the surrounding organs receive the 0% of the dose, a DVH has to be calculated (Fig. 1.3).

While displaying the per cent volume versus dose is more popular, it is useful in some circumstances to plot the absolute volume versus dose. The constraints in table 1.1 updated

to 01/12/14, according to RTOG (Radiation Therapy Oncology Group)1005 of the 05/06/13, have to be respected for the breast.

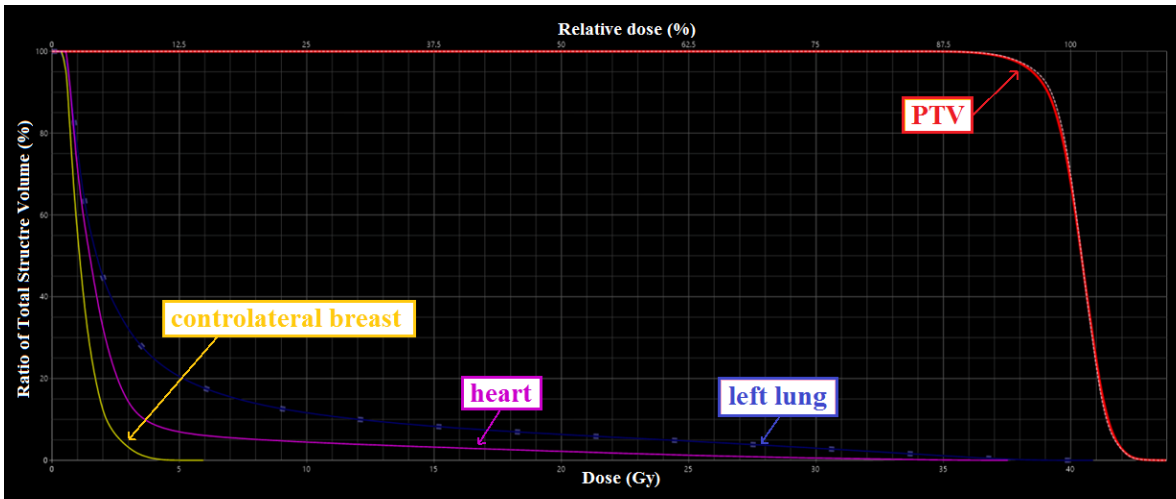


Figure 1.3: Screenshot of a DVH from the TPS graphical interface. Inserts show the name of the organ for each line in the DVH.

Table 1.1: Constraints for the breast updated to 01/12/13 (RTOG 1005 of 05/06/2013). For each organ maximum target dose (D_{MAX}) and mean target dose (D_m) are reported. $V_{16} \leq 5\%$ means that 16% of the heart volume have to receive less than 5% of the dose, similarly for other constraints. Please note that the protocol here adopted is the one of the San Raffaele Hospital which consists of 40 Gy in 15 fractions of 2.667 Gy per fraction.

Organ	Optimal constraint	Acceptable constraint
Breast	$D_{MAX} \leq 43.2 \text{ Gy (108\%)}$ $V_{24\text{Gy}} (= 105\%) \leq 5\%$	
Heart	$V_{16} \leq 5\%$ $V_8 \leq 30\%$ $D_m = 320 \text{ cGy}$	$V_{20} \leq 5\%$ $V_8 \leq 35\%$ $D_m = 400 \text{ cGy}$
Ipsilateral lung	$V_{16} \leq 15\%$ $V_8 \leq 35\%$ $V_4 \leq 50\%$	$V_{16} \leq 20\%$ $V_8 \leq 40\%$ $V_4 \leq 55\%$
Contralateral lung	$V_4 \leq 10\%$	$V_4 \leq 15\%$
Contralateral breast	$D_{MAX} = 240 \text{ cGy}$ $D_{5\%} = 144 \text{ cGy}$	$D_{MAX} = 384 \text{ cGy}$ $D_{5\%} = 240 \text{ cGy}$
Thyroid	$D_{2\%} = 0.96 \text{ Gy}$	$D_{2\%} \leq 1.44 \text{ Gy}$

1.1.2 Direct planning: 3D-CRT

Direct planning 3D-CRT is normally delivered with two opposed tangential fields to encompass the breast, often including part of the chest wall and the axilla. The treatment planning consists in designing the radiation fields based on CT data sets from the individual patient. In order to better conform the PTV the multileaf collimator of the Linac has to be

properly positioned. If positioned too near to the boundaries, penumbra areas are created thus preventing the PTV from being completely irradiated. In addition, specific consideration has to be given to the fact that the inspiration can create PTV modifications and for this reason the multileaf collimator had to be positioned towards the external side of the breast to try conforming the PTV as much as possible.

To ensure dose homogeneity, two extra elements can be used:

- Two reinforcement fields, opportunely weighted to uniform dose distribution. These two fields are equal to the principal fields, but they are much less weighted and they could have a different multileaf collimator position. In this way they can cover dose accumulations and irradiate underdosed areas.
- Two wedges with high atomic number manually applied by the technicians at the exit of the beam (Fig. 1.4). The beam hardening effect causes the areas of the breast furthest from the beam to be able to take more dose than they would take in the absence of the wedges.

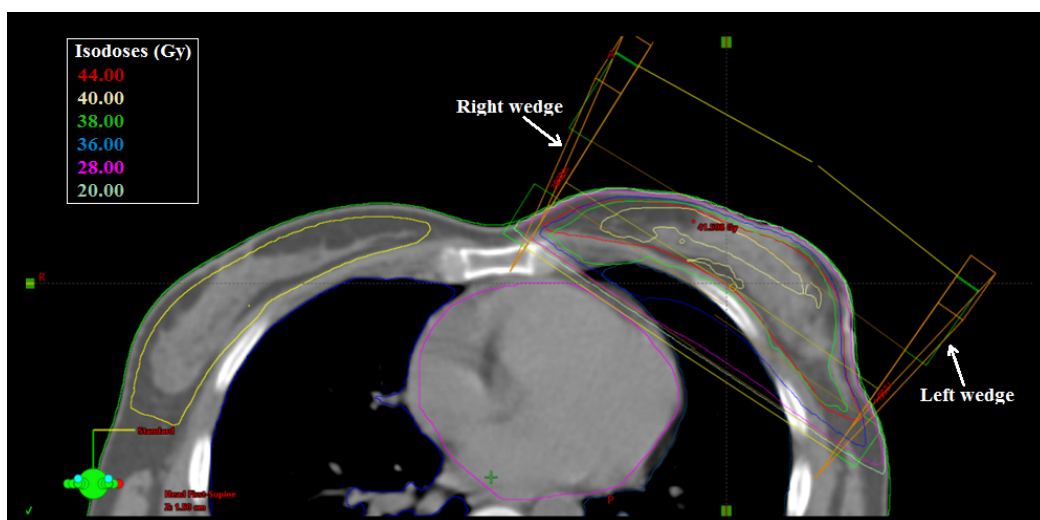


Figure 1.4: Screenshot of the TPS graphical interface, in transversal view: two wedges are positioned in the positions of the two tangential fields. Insert shows the isodose curves.

In 3D-CRT, the irradiation is static, i.e. fields and multileaf collimator are static, and it occurs to the same source-to-axis distance (SAD) for both fields. The beam is placed in the position of the first field and irradiates the breast, then the first reinforcing field starts, possibly with the multileaf collimator in a different position and the addition of a wedge. Then the beam shuts off, puts itself in the position of the second field and irradiation starts again. In the end there is the second reinforced beam. The whole process is quite slow and takes several minutes. 3D-CRT (Fig. 1.5) strength is on how accurate the PTV is and how good the dose distribution is with respect to the prescription dose.

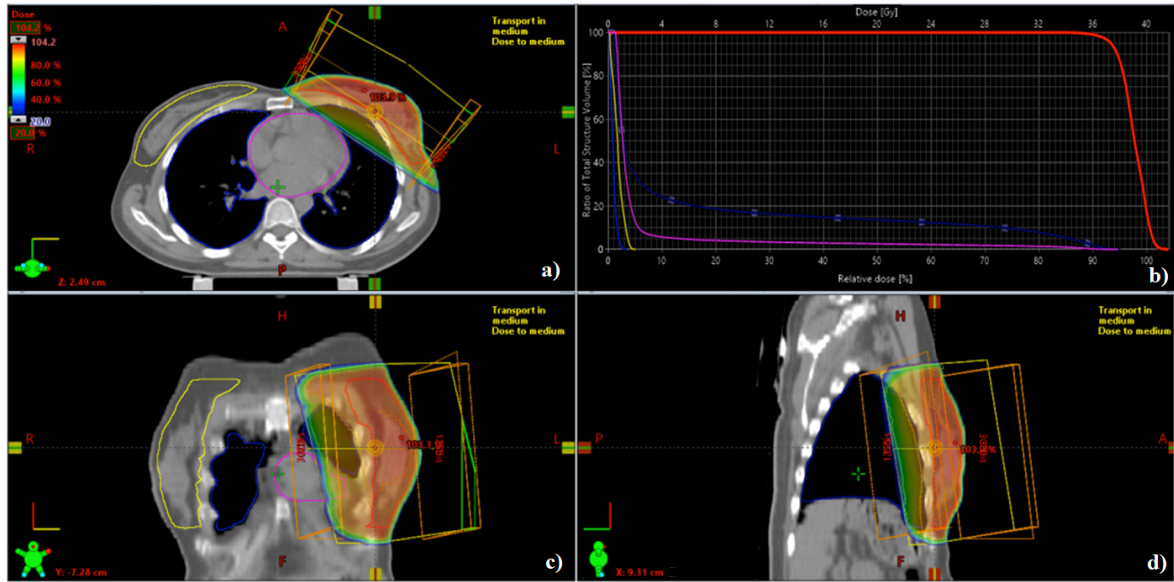


Figure 1.5: Screenshot of an approved treatment plan for a left breast in the TPS graphical interface, realized with 3D-BRT. a) transversal view, b) DVH, c) frontal view, d) sagittal view.

1.1.3 Inverse planning: VMAT

The inverse planning VMAT (Volumetric Modulated Arc Therapy) also called Rapid Arc, is a treatment using a medical linear accelerator and modulated radiation beams moving along arcs able to target with millimetric precision the maximum dose to the tumour, sparing the organs at risk. VMAT was introduced in clinical practice in 2008 after the publication of the seminal work of Otto which opened the road to the implementation of VMAT optimization algorithms in the treatment planning systems [8]. One of the specific features of VMAT is the possibility to perform a cone-beam CT with the purpose to control and correct patient position before each radiotherapy session. The irradiation is not static as the beam is rotating and for each irradiation angle the dose rate and the beam shape can change due to the multileaf collimator motion (Fig. 1.6).

Since with this treatment planning the DVH are designed instead of the radiation fields, it is necessary to create three other structures:

- the “target”, which is consisting of PTV plus 0.7 cm towards the external to take into account the inspiration;
- the “ghost”, also called shell, a non-real structure (about 3-cm thick) positioned behind PTV to protect organs at risk;
- the “virtual bolus”, a non-real structure positioned over the skin, to simulate a plastic material (1.01 g/cm^3 dense, about 0.5-cm thick) and guarantee the optimization of the treatment plan conforming the dose to the target.

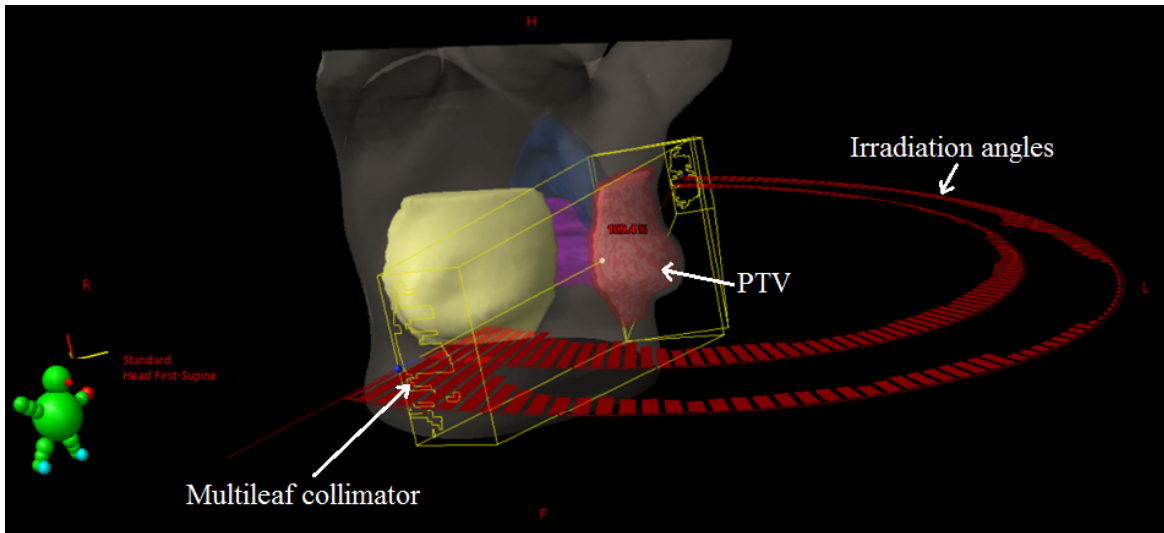


Figure 1.6: Screenshot of the TPS graphical interface. In the first plane there is the shape of the multileaf collimator while rotate along the irradiation angles. Rotation axis is centred in the PTV.

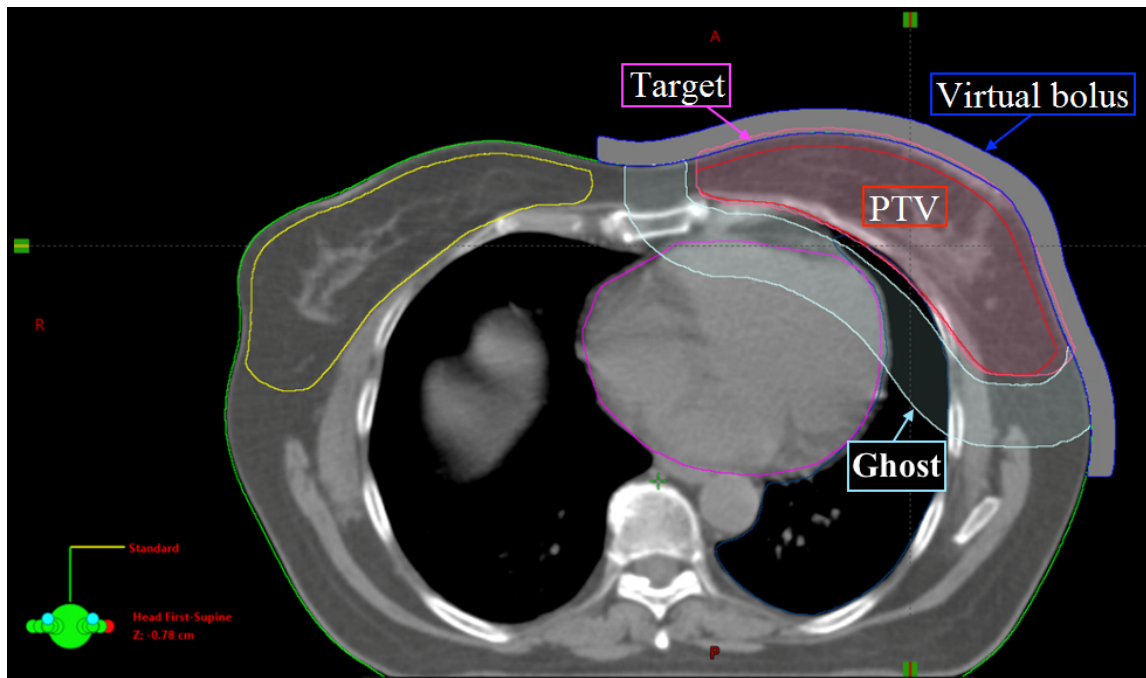


Figure 1.7: Screenshot of the TPS graphical interface in transversal view. Virtual bolus, target, PVT and ghost are depicted.

At this point it is the turn of DVH estimation. It is possible to work on target (no more on the PTV) and other organs at risk. For each organ, DVH has to respect the dose constraints reported in table 1. When DVHs are finished, an automatic simulation is started to calculate the final dose to the organs. In the first three levels of the simulation it is possible to change values in the DVHs, forcing the algorithm to lowering the doses for the organs at risk. In the fourth level the optimization process finishes and isodose curves are ready (Figs. 1.8 and 1.9).

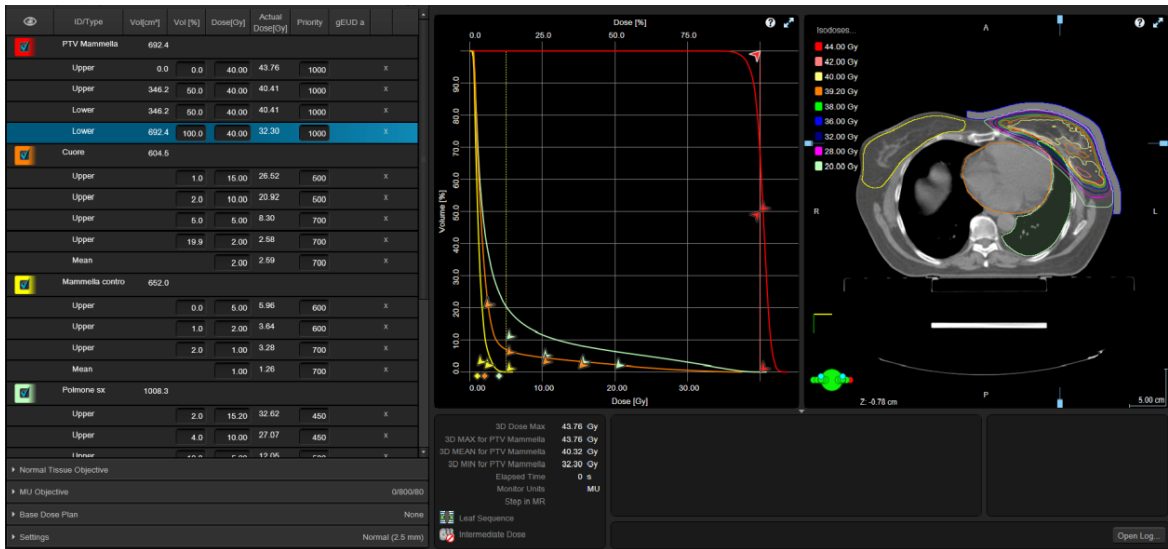


Figure 1.8: Screenshot of the TPS graphical interface. On the left there is the part where it is possible to insert the constraint values manually, in the centre there is the estimated DVH, on the right there is transversal view of the patient organs with isodoses curves.

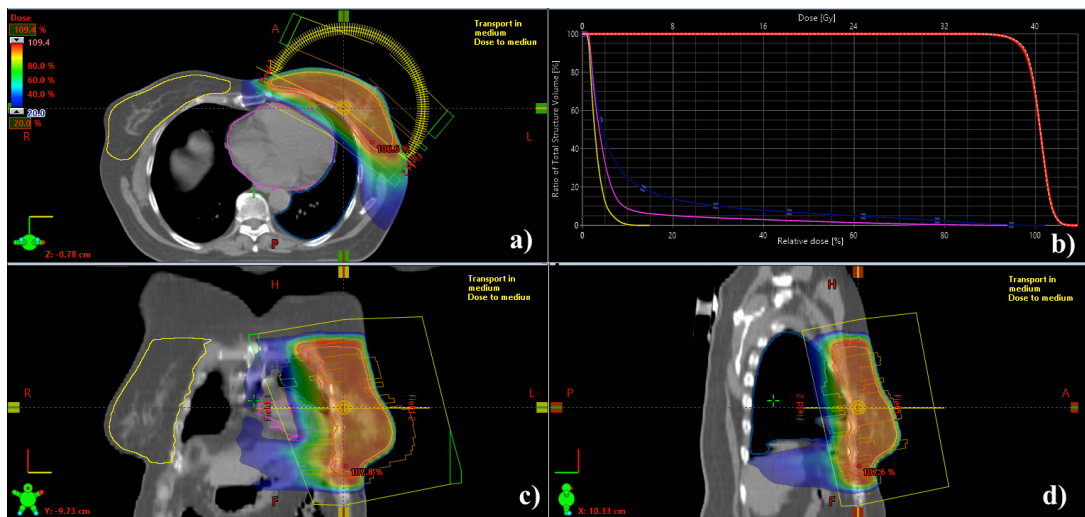


Figure 1.9: Screenshot of the completed treatment plan for a left breast in the TPS graphical interface, realized with VMAT. a) transversal view, b) DVH, c) frontal view, d) sagittal view.

Comparing 3D-CRT and VMAT:

- Choosing between 3D-CRT and VMAT is the radiation oncologist task. In general, it depends on patient anatomy, i.e. if lung is too close to the breast, VMAT is preferable due to its capability of better conform the dose to the tumour and an improved sparing of organs at risk;
- Compared to the 3D-CRT, the VMAT allows to better conform the dose to the tumour in the range of high doses (> 10 Gy), although low dose curves reach wider areas with higher risk of secondary cancer induction or lifetime risk. In 3D-CRT it is the opposite;

- For this reason, the choice between the two techniques also depends on the patient age due to the insurgence of secondary tumours at low doses with VMAT technique;
- In 3D-CRT the patient undergoes two low dose radiographies, whereas VMAT contemplates a cone beam CT, at a higher dose, which must be taken into account in the TPS;
- VMAT is generally much simpler and faster compared to 3D-CRT because there are no wedges.
- For both cases, when the TPS is finished, the optimization of a treatment plan has to be evaluated not only in terms of dose distribution, but also in terms of dose–response characteristics of the given disease and the irradiated normal tissues. In fact biologic response of the tumour and the normal tissues need to be considered.

Summarizing, VMAT ensures target coverage, homogeneity and optimal conformality, it is applicable to whole breast or partial breast treatments. To improve this technique the use of advanced photon beams (the high intensity or flattening filter free beams) was tested and the results suggest that improved sparing of organs at risk, can be achieved, particularly at low doses.

1.2 Partial breast Irradiation (PBI)

Partial breast irradiation (PBI) is a technique developed to improve breast cancer radiotherapy. After a lumpectomy for early stage, there is the possibility to irradiate a limited volume of breast tissue. PBI has been delivered via interstitial brachytherapy, intracavitary brachytherapy, intraoperative radiation therapy, or 3-dimensional external beam radiation therapy (3D-EBRT). The benefits of this technique are: reduced treatment volumes, reduced dose to organs at risk, improved cosmesis [6].

1.3 Accelerated Partial Breast Irradiation (APBI)

Accelerated partial breast irradiation (APBI) refers to PBI with a shortened treatment duration by using a higher dose of radiation per fraction. APBI can be delivered via the following techniques: interstitial brachytherapy, intra-cavitary brachytherapy, 3-dimensional (3D) conformal external beam radiation therapy (EBRT), and intraoperative radiation therapy (IORT). Usually PBI has commonly been delivered during more than 5 days, twice daily in 10 fractions, so the treatment length is highly reduced. Interstitial brachytherapy involves inserting temporary catheters into the surgical cavity and

surrounding tissue to deliver high-dose-rate brachytherapy. Intracavitary radiation therapy involves placing a temporary catheter into the lumpectomy cavity, typically secured by inflating a balloon or a strut based applicator, and then applying high-dose-rate sources into the intracavitary implant. Both intracavitary and interstitial brachytherapy are semi-invasive techniques in which the radiation is being emitted internally and that could cause infections, wound healing delays and scarring post insertion of implants. Balloon-based brachytherapy applicators may not be optimal for patients with cavities close to the skin or with irregular shaped cavities. In intracavitary and interstitial therapy the radiation is being emitted internally [6].

1.4 Stereotactic Partial Breast Irradiation (S-PBI)

Stereotactic body radiation therapy (S-BRT) consists in large doses of radiation in few fractions. In 2009 Bondiau et al proposed the use of stereotactic radiation therapy for breast cancer employing robotic radiosurgery with the Cyberknife (Accuray, Sunnyvale, CA). With a computer tomography (CT) scan is possible to contour the gross tumour volume (GTV), from GTV clinical target volume (CTV) is calculated by adding 5 mm margin. Finally, the planning target volume is $PTV = CTV + 2 \text{ mm margin}$. Regarding dosimetry, the maximum dose accepted is 15 Gy to 10 cm^3 of the skin and chest wall, and 5 Gy to 5 cm^3 of the lung. Dose to the skin is 10%-30% of the prescription dose [9].

Swedish Medical Center in Seattle and Winthrop University Hospital published results of patients whom received stereotactic partial breast radiation (S-PBI) with Cyberknife. Twenty-one patients were treated with doses ranging from 25–36 Gy in 5–10 fractions, other 26 patients were treated with 30 Gy divided into 5 fractions (Fig. 1.10). To immobilize the breast, patients were positioned or with a thermoplastic cast across the chest with a hole around the areola, or in an alpha cradle with a support bra, or in natural breast position. The cosmesis was good in all patients, and there was no high toxicity [10] [11].

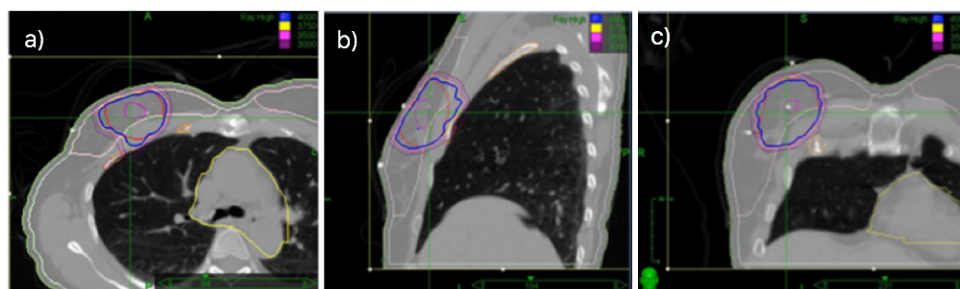


Figure 1.10: Right breast 40 Gy in 5 fractions S-PBI plan depicting (a) axial, (b) sagittal and (c) coronal plans of view [6].

1.5 Kilovoltage Rotational Radiotherapy with X-ray tube (kV-EBRT)

Dedicated breast computed tomography (bCT) is an experimental tomographic cone-beam X-ray-based imaging modality that generates three-dimensional (3D) images of the pendant breast. In 2012 J. Boone (University of California Davis) proposed and demonstrated the feasibility of a bCT platform to deliver rotational kilovoltage (kV) external beam radiotherapy (RT) for partial breast irradiation, whole breast irradiation, and dose painting [12]. The external-beam rotational radiotherapy (kV-EBRT) of the breast cancer is possible with an orthovoltage X-ray tube with the capability of rotate around the breast – the axis of rotation of the gantry goes through the tumour site. The technique could be implemented using a rotating gantry of a cone-beam computed tomography scanner dedicated to the breast [13], in this way a precise 3D localization of the tumour is possible.

The bCT platform was designed for diagnostic breast imaging, thanks to this characteristic it is also capable of kV-EBRT positioned for image-guided RT. In this platform the patient is prone on a rotational/translational bed with a hole for the pendent breast, the orthovoltage X-ray tube stays under the bed in a dedicated gantry and can rotate around the breast (Fig. 1.11). A geometry like this allows to overcome one of the most important problems of conventional radiotherapy: the dose to the organs at risk like heart and lungs. In this way is possible to reduce the incidence of ischemic heart disease, atherosclerosis and radiation-induced lung cancer.

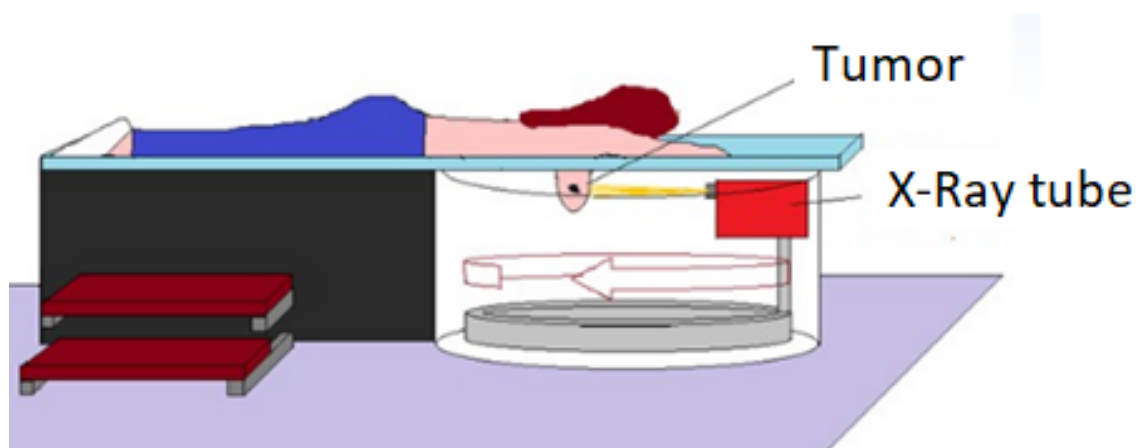


Figure 1.11: The X-ray tube rotating around the breast below the patient bed allows to irradiate the tumour along a full arc, while permitting also to acquire CT projections for bCT on the same platform (from: De Lucia P. A. Presented at National Congress of the Italian Society of Physics, Rome, Italy, 25/09/2015).

The advantages of the kV-EBRT technique with respect to conventional radiotherapy are:

- the bCT platform is smaller and easier than the linear accelerator of the conventional breast radiotherapy, moreover it does not require a bunker, so it is also cheaper;
- reduction of patient repositioning error and improvement in treatment accuracy;
- the use of a prone rather than a supine patient position;
- possibility of simultaneous imaging during treatment;
- thanks to rotational summation of a collimated kV beam, dose sparing to the skin comes out to be equivalent to what megavoltage photons can get with the build-up effect.

When the collimated X-ray beam irradiates the breast in a full rotation, the summation of the dose deposited ensues in a dose distribution peaked at the centre of rotation. The width and shape of the peak depend on the beam collimation on the horizontal plane, while the longitudinal height of the irradiated target (in the direction from chest wall to nipple) depends on the vertical collimation. This proposal has been evaluated using a Monte Carlo simulations, which demonstrated the potential for PBI, dose painting, and WBI with skin sparing with kV-EBRT at about 320 kV.

Moreover, there is the possibility to treat small volumes. This is realizable with a highly collimated X-ray beam rotating around the isocentre and depositing a focus of dose with rapid dose falloff to the surrounding medium. In this way the breast skin receives a small fraction of the dose, as demonstrated by a 1-cm beam delivering <7% of the maximal dose to the skin. To realize dose painting, a narrow beam has to do multiple rotations around different centres of rotation. Finally, whole breast irradiation (WBI) is done rotating several times while varying beam collimation widths and intensities. Better homogeneity can be achieved with further collimation widths. The clinical feasibility of WBI require a bCT platform with a dynamic multileaf collimator, an X-ray source capable of rapid tube current modulation, and a slip-ring gantry design for continuous source rotation.

An important topic for both PBI and WBI realized with kV-EBRT is the total treatment time. The bCT platform needs a high-power tube capable of delivering sufficient dose rates. For 320-kVp source, a dose rate of 1 Gy/min at a 50-cm source-to-surface distance (SSD) is realizable. In conventional EBRT with megavoltage photon the dose rate is about 500 cGy/min, so the treatment time is about 2 min, but considering patient and source positioning, the total time can arrive to 15 min. For kV-EBRT the beam-on time is longer, but patient and source positioning is simpler so the total time is comparable.

1.4 Synchrotron Radiation Rotational Radiotherapy for breast cancer (SR³T)

In 2016 De Lucia et al. proposed to come out EBRT for breast cancer using a monochromatic synchrotron radiation (SR) beam and a dedicated setup for irradiating the pendant breast (SR-EBRT) [14]. The irradiation geometry is the same of kV-EBRT, but instead of an orthovoltage X-ray tube, the source is a SR beam of equivalent or lower effective photon energy than for 320 kVp. To give the highest dose at the isocentre and ensure enough skin sparing, the vertical axis of rotation is centred at the tumour (Figs. 1.12, 1.13). During the scan the breast should be immobilized. The advantage is that the SR beam allows a monoenergetic X-ray beam with energy in the range 60–120 keV and with higher flux and lower energy [15]. The technique is named Synchrotron Radiation external beam Rotational Radiotherapy (SR³T) and could become a possible alternative to conventional radiotherapy of breast cancer, in particularly for boost or small lesion irradiation in few fractions.

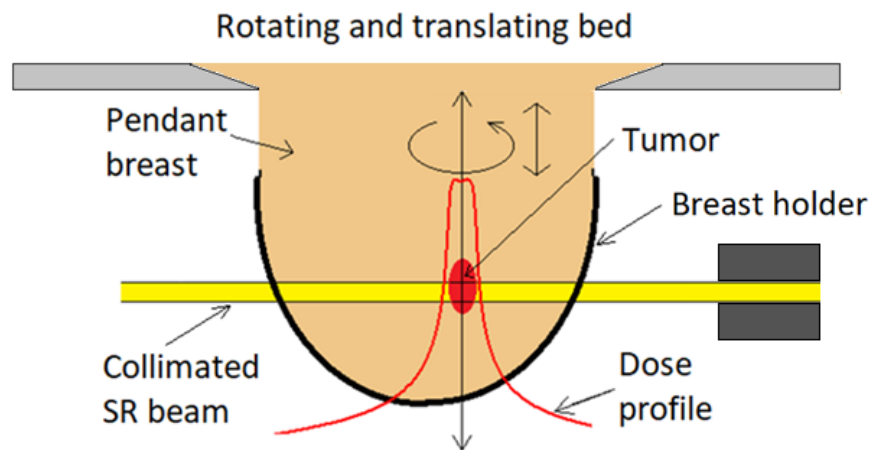


Figure 1.12: Sketch of SR-EBRT. The patient breast is hanging from a hole, while the bed is rotating around a vertical axis centred in the tumour. The collimated X-ray beam from a SR source irradiates the tumour [3].

A dedicated Geant4 Monte Carlo simulation code was developed to validate this technique and assess the skin sparing effect in terms of centre-to-periphery dose ratio at energies from 60 keV to 175 keV. The code compares literature and measurement with breast phantom with a polychromatic X-ray beam, and as result shows a 7:1 to 10:1 tumour-to-skin ratio from 60 keV to 175 keV, these values are satisfactory for radiotherapy. Furthermore the simulations show that the periphery-to-centre dose ratio at 60 keV is 14%, comparable with the 10% value obtained by a polyenergetic beam produced at 300 kVp with an orthovoltage X-ray tube, and acceptable to that of conventional radiotherapy [15].

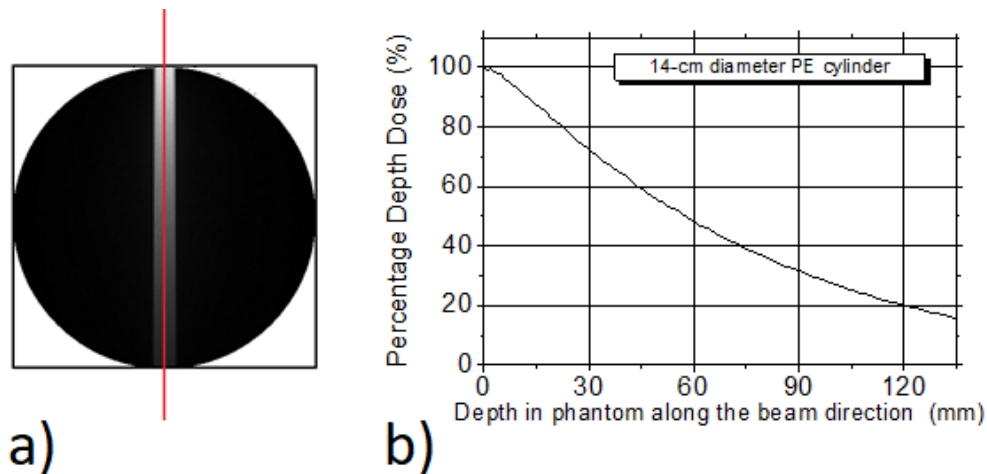


Figure 1.13: a) Coronal slice through a 3D map of absorbed dose for a 100 keV collimated X-ray beam (incident from top to bottom in the figure): the grey level is proportional to the absorbed dose, so that the figure shows the decreasing dose with depth in the 14-cm diameter polyethylene cylindrical phantom. b) Dose line profile along the direction of the red line shown in a). For this single-view irradiation, the dose has a maximum at the entrance surface of the phantom. [3]

The likelihood of realizing dose-painting with multiple rotations was demonstrated irradiating EBT3 radiochromic films in a phantom and collimating the SR beam at 1.5 cm in the horizontal direction. Different radial dose distributions are feasible in dependence of the beam size, and varying the beam collimation both whole breast as well as partial breast irradiation can be performed.

The idea is to use a SR beam with photon down to 60 keV for SR-EBRT of breast cancer, with a skin sparing factor (dose to the skin divided by dose to the tumour) close to that of orthovoltage EBTR at 320 kVp. The technique foresees the injection of gold nanoparticle – used as radio-sensitizers – or iodinate solutions at low energy (60–80 keV), which allow dose-enhanced breast SR-EBRT and BCT for image-guided radiotherapy. The photoelectric absorption increases for kilovoltage energies with respect to MV energies in the sites where these agents accumulate. Regarding treatment time, several minutes occur so that the patient bed rotate and translate to cover all the tumour volume. This time is comparable with that of conventional radiotherapy [15].

Initial measurements were performed at the Australian Synchrotron facility (Clayton, Victoria, Australia).

Chapter 2

Experimental validation of the SR³T technique

2.1 Dose distribution in breast phantom at 100 keV with synchrotron radiation

Measurements were performed at the Australian Synchrotron (AS), Clayton (Melbourne), Australia, at the Imaging and Medical Beamline (IMBL) on August 2017 by the medical physics group of Università di Napoli Federico II, within an experimental project approved by the Scientific Committee of the AS. While it was not possible for me to participate to these measurements, I participated to the preliminary measurements in the laboratory, in particular I analysed the radiochromic film dosimetry. The investigation on the feasibility of SR³T was done at 100 keV [3].

2.1.1 Radiochromic film dosimetry at 100 keV

Radiochromic films represent a powerful two-dimensional (2D) dosimetry instruments for radiotherapy treatment verification and quality assurance test are represented by. They are near tissue-equivalent and can map absorbed dose by a self-developing radiation-induced colour change, determined by the presence of organic di-acetylene monomers (which polymerize under irradiation). Radiochromic dosimetry films (GAFCHROMIC™ films) type EBT3 (Ashland Inc., Covington, KY, USA) can be used in the dose range: 0.1 Gy to 20 Gy. The acronym EBT stands for External Beam Therapy. They are made of two layer of matte polyester of 125 μm and in the centre there is an active layer of 20 μm made by a matrix throughout which monomer (and dye) particles are uniformly distributed (Fig. 2.1). Silica particles are added in polyester layer to avoid Newton rings.

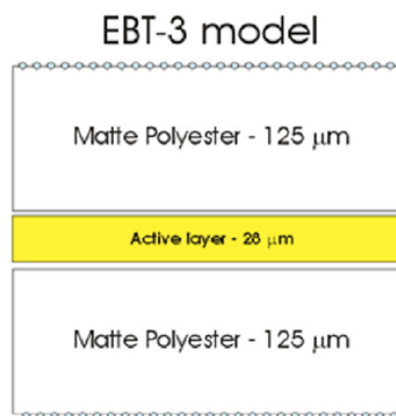


Figure 2.1 Composition of the EBT3 model of GAFCHROMIC™ [16].

Response of the film to radiation is expressed in terms of optical density change, then it is possible to obtain absolute doses thanks to a calibration curve established during the calibration process with a reference beam quality of known dose rate and under specific conditions. We adopted the same protocol as in *Devic et al.* [16].

EBT3 films (lot #05181501) were cut into $3 \times 6 \text{ cm}^2$ (for the calibration curve) and $4 \times 20 \text{ cm}^2$ (for the 2D dose maps) pieces. To measure change in their response, before and after irradiation, each film was placed always in the same position at the centre of the flatbed scanner EPSON V850 PRO, using a paper template. EPSON Perfection V850 Pro is a flatbed scanner with scanning resolution of 6400 dpi (H \times V), with a Matrix CCD with Micro Lens and High Pass Optics as optical sensor, and White LED, IR LED with ReadyScan LED Technology as light source (Fig. 2.2).



Figure 2.2: EPSON V850 PRO scanner.

Films were scanned in transmission mode. Three different 48-bit RGB (72 dpi) scans were obtained both pre- and post-irradiations, and saved as tagged image file format (TIFF) image files. Since the polymer created after irradiation has the highest absorption in the red part of the optical spectrum, centred at the wavelength of 633 nm, the images were analysed in the red channel (16-bit), sampling raw data from 3 different regions of interest (ROI) of $1 \times 1 \text{ cm}^2$, that is $28 \times 28 \text{ pixel}^2$ (Fig. 2.3) as the average pixel value (PV) and its corresponding standard deviation (σ_{PV}).

Since each film piece was scanned three times consecutively, there are three values of PV and σ_{PV} for each ROI: PV_i^j and $\sigma_{PV_i^j}$, where $i = 1, 2, 3$, is the index of the ROI as indicated in fig. 2.4, $j = 1, 2, 3$, is the scanning index. In order to reduce the noise, a weighted average for each ROI is calculated.

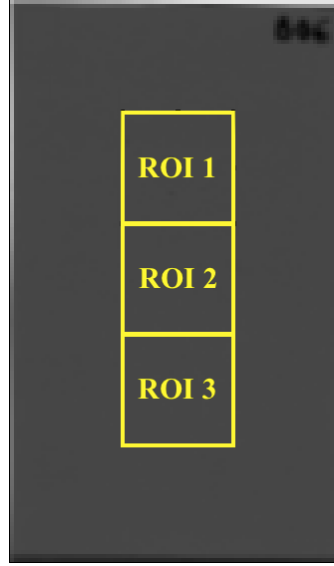


Fig 2.3: EBT3 film piece exposed at 6 Gy dose value. ROIs 1-3 indicate the regions where raw pixel data are acquired and pixel value and its standard deviation are calculated.

The average pixel value, PV_i , is calculated using a weighted mean of the 3 sampled ROIs:

$$PV_i = \sum_{j=1}^3 [\omega^j \cdot (PV_i^j)] \quad (1)$$

with the corresponding normalized weights, ω^j , calculated as:

$$\omega^j = \frac{1/(\sigma_{PV_i^j})^2}{\sum_{j=1}^3 [1/(\sigma_{PV_i^j})^2]} \quad (2)$$

and the corresponding standard deviation on PV_i , σ_{PV_i} , is:

$$\sigma_{PV_i} = \sqrt{\frac{3}{\sum_{j=1}^3 [1/(\sigma_{PV_i^j})^2]}} \quad (3)$$

For the 16-bit depth images, the minimum value would correspond to 0 and the maximum would be $2^{16} = 65535$. The response of radiochromic films to radiation is described by transmittance (the transmitted light intensity relative to initial intensity), T :

$$T = \frac{I_{\text{trans}}}{I_0} = \frac{PV_{\text{trans}}}{2^{16}} \quad (4)$$

Since each film piece has an initial transmittance before being irradiated, the quantity of interest in film dosimetry is the actual change of T . It is preferable to use the change in optical density,

$$OD = -\log_{10} T = -\log_{10} \left(\frac{PV_{\text{trans}}}{2^{16}} \right) \quad (5)$$

after irradiation, for every single ROI_{*i*}:

$$\text{netOD}^i = \text{OD}_{\text{after}}^i - \text{OD}_{\text{before}}^i = \log_{10} \left(\frac{PV_{\text{before}}^i}{PV_{\text{after}}^i} \right) \quad (6)$$

If one considers the impact of the dark (or background) signal and the influence of environmental factors (using a control film piece not irradiated), one has:

$$\Delta(\text{netOD}^i) = \log_{10} \frac{PV_{\text{before}} - PV_{\text{bckg}}}{PV_{\text{after}} - PV_{\text{bckg}}} - \log_{10} \frac{PV_{\text{before}}^{\text{control}} - PV_{\text{bckg}}}{PV_{\text{after}}^{\text{control}} - PV_{\text{bckg}}} \quad (7)$$

and the standard deviation:

$$\sigma_{\Delta\text{netOD}^i} = \frac{1}{\ln 10} \sqrt{ \begin{aligned} & \frac{(\sigma_{PV_{\text{before}}})^2}{(PV_{\text{before}} - PV_{\text{bckg}})^2} + \frac{(\sigma_{PV_{\text{after}}})^2}{(PV_{\text{after}} - PV_{\text{bckg}})^2} + \\ & + \left[\frac{PV_{\text{before}} - PV_{\text{after}}}{(PV_{\text{before}} - PV_{\text{bckg}}) \cdot (PV_{\text{after}} - PV_{\text{bckg}})} \right]^2 \cdot (\sigma_{\text{bckg}})^2 + \\ & + \frac{(\sigma_{PV_{\text{before}}^{\text{control}}})^2}{(PV_{\text{before}}^{\text{control}} - PV_{\text{bckg}})^2} + \frac{(\sigma_{PV_{\text{after}}^{\text{control}}})^2}{(PV_{\text{after}}^{\text{control}} - PV_{\text{bckg}})^2} + \\ & + \left[\frac{PV_{\text{before}}^{\text{control}} - PV_{\text{after}}^{\text{control}}}{(PV_{\text{before}}^{\text{control}} - PV_{\text{bckg}}) \cdot (PV_{\text{after}}^{\text{control}} - PV_{\text{bckg}})} \right]^2 \cdot (\sigma_{\text{bckg}})^2 \end{aligned} } \quad (8)$$

The average optical density change is calculated using a weighted mean of the 3 sampled ROIs:

$$\overline{\Delta\text{netOD}} = \sum_{i=1}^3 [w^i \cdot \Delta(\text{netOD}^i)] \quad (9)$$

with the corresponding normalized weights calculated as:

$$w^i = \frac{1/(\sigma_{\Delta\text{netOD}^i})^2}{\sum_{i=1}^3 [1/(\sigma_{\Delta\text{netOD}^i})^2]} \quad (10)$$

and the corresponding standard deviation on $\overline{\Delta\text{netOD}}$:

$$\sigma_{\overline{\Delta\text{netOD}}} = \sqrt{\frac{3}{\sum_{i=1}^3 \left[\frac{1}{(\sigma_{\Delta\text{netOD}^i})^2} \right]}} \quad (11)$$

At IMBL, EBT3 radiochromic films were calibrated in terms of air kerma free-in-air. EBT3 films were positioned in a PMMA frame on a robotic support, capable of translating with a speed of 10 mm/s. The SR beam height was 20.5 mm and the dose rate was of 56.65 mGy/s. So, translating the support several times, the EBT3 films were irradiated and exposed to an air kerma free-in-air in the range of 0.05 Gy to 2.0 Gy.

After the irradiation, PV values were collected and the average optical density change, $\overline{\Delta\text{netOD}}$, and the corresponding standard deviation, $\sigma_{\overline{\Delta\text{netOD}}}$, are calculated and reported in table 2.1.

Table 2.1: Values of average optical density change, $\overline{\Delta_{\text{netOD}}}$, and the corresponding standard deviation, $\sigma_{\overline{\Delta_{\text{netOD}}}}$, for each value of dose.

$\overline{\Delta_{\text{netOD}}} \pm \sigma_{\overline{\Delta_{\text{netOD}}}}$	$D \pm \sigma_D$ (mGy)
0.0061 ± 0.0011	62.4 ± 1.2
0.0069 ± 0.0011	96.6 ± 1.9
0.0218 ± 0.0011	289 ± 6
0.0373 ± 0.0012	479 ± 10
0.0654 ± 0.0011	960 ± 19
0.0954 ± 0.0011	1450 ± 30
0.1195 ± 0.0012	1930 ± 40

Values in the Table 2.1, are used to evaluate the calibration curve. The more suitable function is the power function: $y = a*x + b*x^n$ (Fig. 2.4).

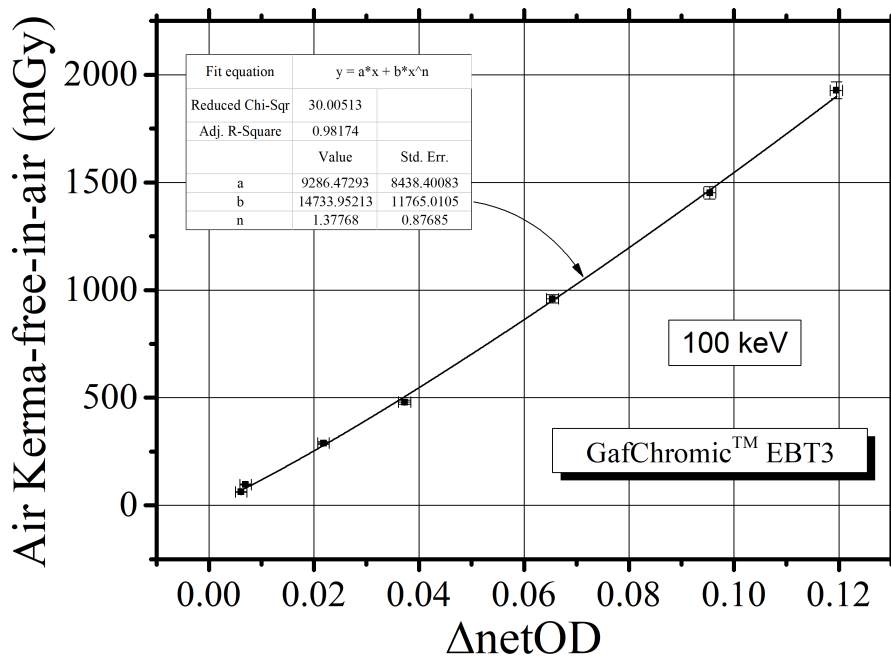


Figure 2.4: Calibration curve for the response of radiochromic film EBT3 at 100 keV. The continuous line is a fit with a power function to the data points.

2.1.2 Measurements in breast phantom at 100 keV

The purpose of the measurements was to estimate the radial dose profile and dose distribution in a breast phantom at 100 keV using radiochromic film EBT3 [3]. This paragraph shows results of this work.

In order to evaluate the radial dose profile, a 14-cm diameter polyethylene (PE) cylindrical phantom was used, and measurements were performed using a Semiflex ionization chamber (PTW 31010) with the dosimeter T10023 UNIDOS weblin (PTW Freiburg, Germany). PE is a good substitute for the adipose tissue in the breast. Results (Fig.

2.5) show the radial dose distribution at beam height of 1.0 cm and different beam widths of 1.5, 4, 5.5, 7, 16 cm. The radial dose distribution depends on the beam collimation. For a beam width of 16 cm, there is a cupped profile, with the minimum at the centre of the phantom and the maximum at the periphery. On the contrary, for smaller beam collimations, the cupping profile shrinks and the radial dose distribution presents a peak at the centre of rotation. The experiment was also simulated with the MC code, and simulations agreed with the experimental data. The dose ratio decreases by narrowing the beam width, because of the principle of rotational summation of the dose. Periphery-to-centre dose ratio ranges between 11.9% and 156% at 6.5 cm, for beam collimation of 1 cm and 16 cm, respectively.

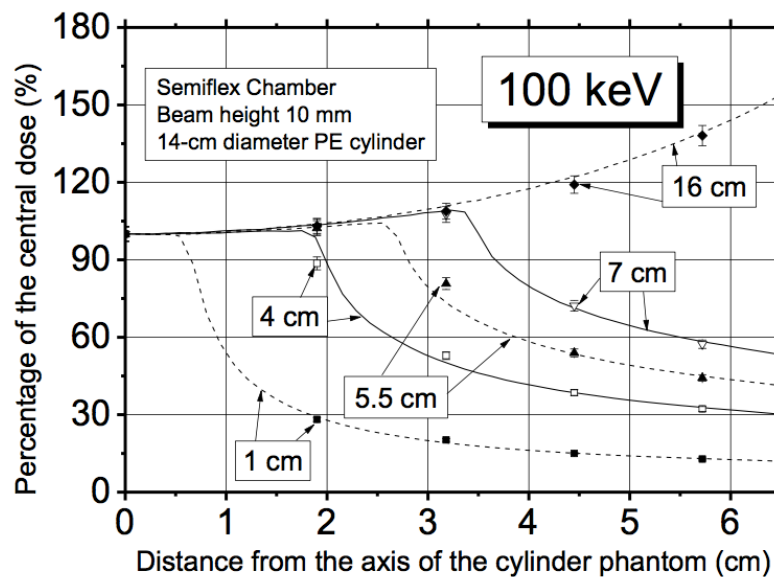


Figure 2.5: Comparison between measured (symbols) and simulated (lines) air kerma values in the PE cylindrical phantom for beam width of 1, 4, 5.5, 7, 16 cm at 100 keV [3].

The dose distribution was evaluated using a 14-cm diameter PMMA cylindrical phantom and by inserting EBT3 radiochromic film at its mid-plane, in order to have a 2D dose map produced by the irradiation of a target volume at the centre of phantom. The SR beam size was 1.5 cm × 1.0 cm (H × W). The phantom rotated by 360° during the irradiation. Results show a peaked distribution in the centre of rotation, with a peak of 1.5-cm width at 85% of the maximum dose, due to the principle of dose summation. Outside the target the air kerma values exponentially decrease with the distance from the axis of rotation (Fig. 2.6).

The dose distribution was also evaluated in the whole phantom volume by placing three radiochromic pieces at mid-plane in the phantom. An X-ray beam of size 1.5 × 2.0 cm² (H × W) irradiated the phantom with a target dose of 7 Gy, during a complete rotation of the phantom.

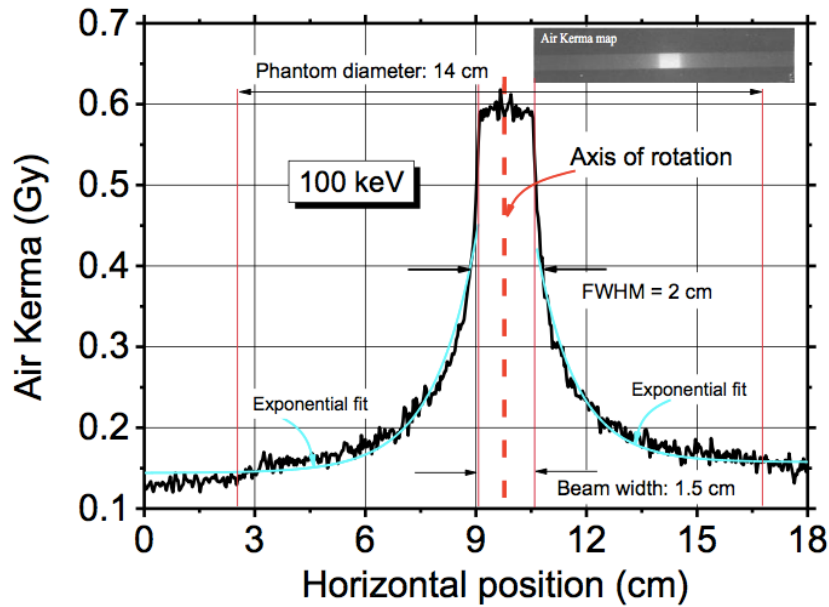


Figure 2.6: Dose profile along the centre of the PMMA phantom. The beam size was 1.5 cm \times 1.0 cm (H \times W). The inset shows the 2D air kerma map imaged by EBT3 film. The cyan continuous lines are exponential fits [3].

The 2D dose map at 100 keV is shown in fig. 2.7 and the isodose curves are showed in fig. 2.8. Scattered radiation produces that a dose from 2% and 10% of the maximum value, even in the areas not directly irradiated by the X-ray beam.

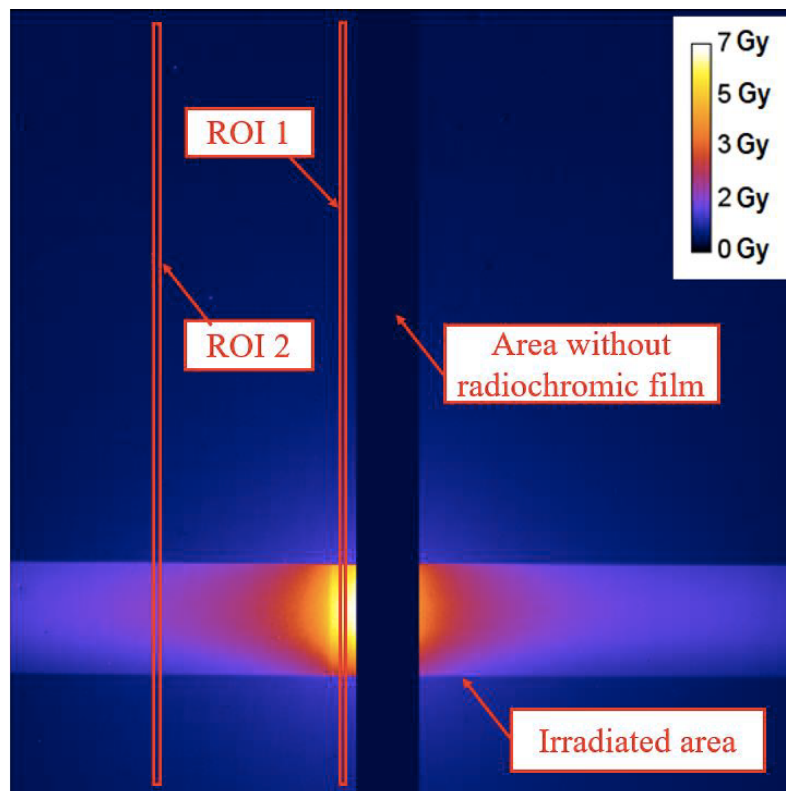


Figure 2.7: 2D dose map at mid-plane in a PMMA phantom at 100 keV. The pixel values indicate values of air kerma free-in-air (Gy) [3].

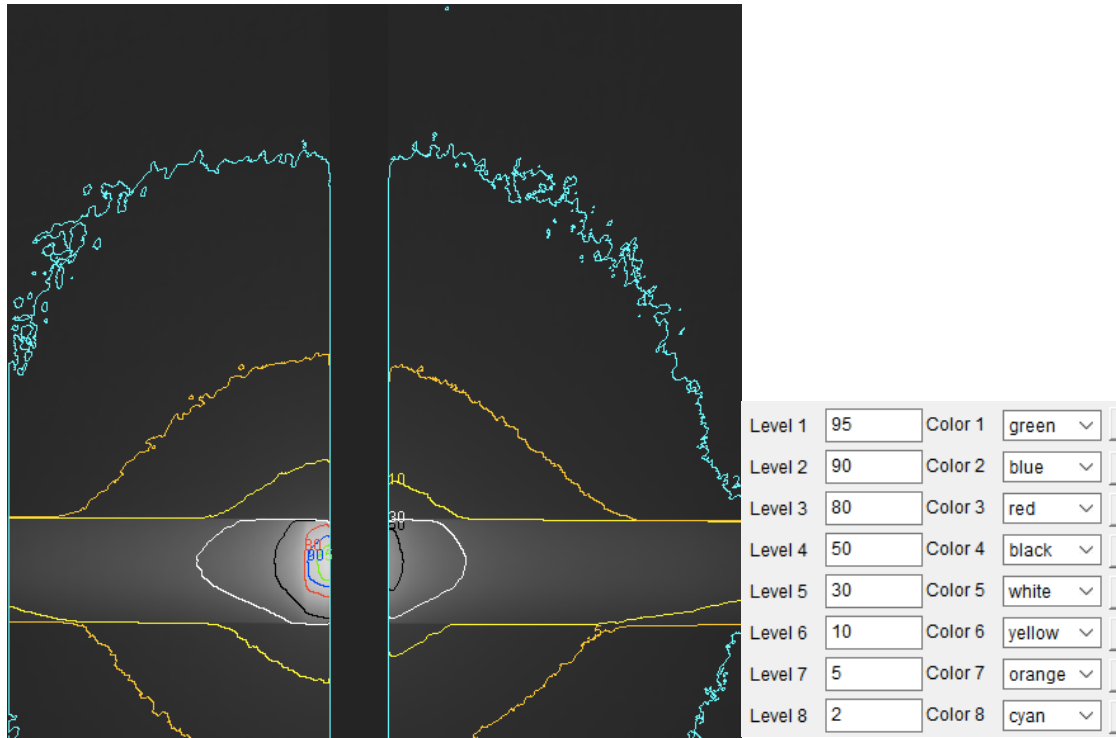


Figure 2.8: Isodose curves obtained in a PMMA phantom at 100 keV. The pixel values were normalized to the maximum. The panel on the right side indicate the isodose legend in percent of the maximum dose [3].

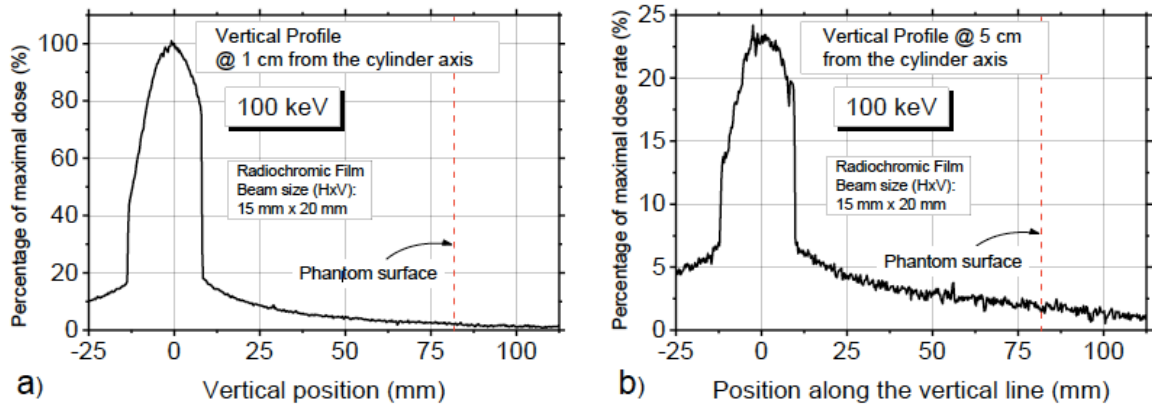


Figure 2.9: Vertical profile evaluated in the dose map at 1 cm, ROI 1 in fig. 2.7 (a), and 5 cm, ROI 2 in fig. 2.7 (b), from the cylinder axis [3].

Figure 2.9 shows the normalized line profiles along the vertical direction evaluated at 1 cm (ROI 1 of Fig. 2.7) and 5 cm (ROI 2 of Fig. 2.7) from the cylinder axis. A peak is present in the area directly irradiated by the primary beam. At 1 cm from the axis, the peak value is the 100% of the target dose, while at 5 cm the peak value is 23% of the target dose. The dose evaluated at 5 cm from the beam centre position in the vertical direction was about 5% of the maximum value in ROI 1 and 3% of the maximum value in ROI 2.

2.2 Dose distribution in breast phantom at 6 MV with VMAT

This paragraph reports the measurements performed during this thesis at San Raffaele Hospital in Milan, Italy, compared with measurements previously performed at the Australian Synchrotron.

2.2.1 Radiochromic film dosimetry at 6 MV

Radiochromic film dosimetry was performed with the aim of reproducing the geometry of the Australian measurements. The only differences are film dimensions and the scanner type. EBT3 films were cut into $3 \times 5 \text{ cm}^2$ (for the calibration curve) and $8 \times 20 \text{ cm}^2$ (for the 2D dose maps) pieces. Films were scanned with the flatbed scanner EPSON Expression 11000XL. It is an A3 scanner with scanning resolution of $2400 \times 4800 \text{ dpi}$ (H \times V), optical density of 3.8 DMax and a Xenon fluorescent lamp as light source. The included software is Epson Scan, SilverFast Ai 8 (Figs. 2.10 and 2.11).



Figure 2.10: Photo of EPSON Expression 11000XL



Figure 2.11: EBT3 film piece positioned in the scanner with the help of a paper guide.

2.2.2 Eclipse™ TPS for phantom irradiation

The software used for treatment plans depends on the radiotherapy machine as each machine is provided with its own software. At HSR a Varian LINAC is installed and the *Eclipse™ treatment planning system* is the software used, with an intuitive Windows-based interface. It is an integrated and comprehensive system supporting radiation treatment such as photon, FFF (flattening filter free) beams, electrons, external beams, low-dose-rate brachytherapy and cobalt therapy [18]. All patient data are loaded into this software: imaging data, clinical data and dose prescription. Then, fields and beam arrangements are designed. One of the most useful features of these systems is the computer graphics, which allows beam's-eye-view (BEV) visualization of the targets. The BEV is the plane perpendicular to the central axis of the beam, as if being viewed from the point of the radiation source. Using the BEV option, field margins (distance between field edge and the PTV contour) may be set to cover the PTV within a sufficiently high isodose level, thanks to the positioning of the multileaf collimator (Fig. 2.12).

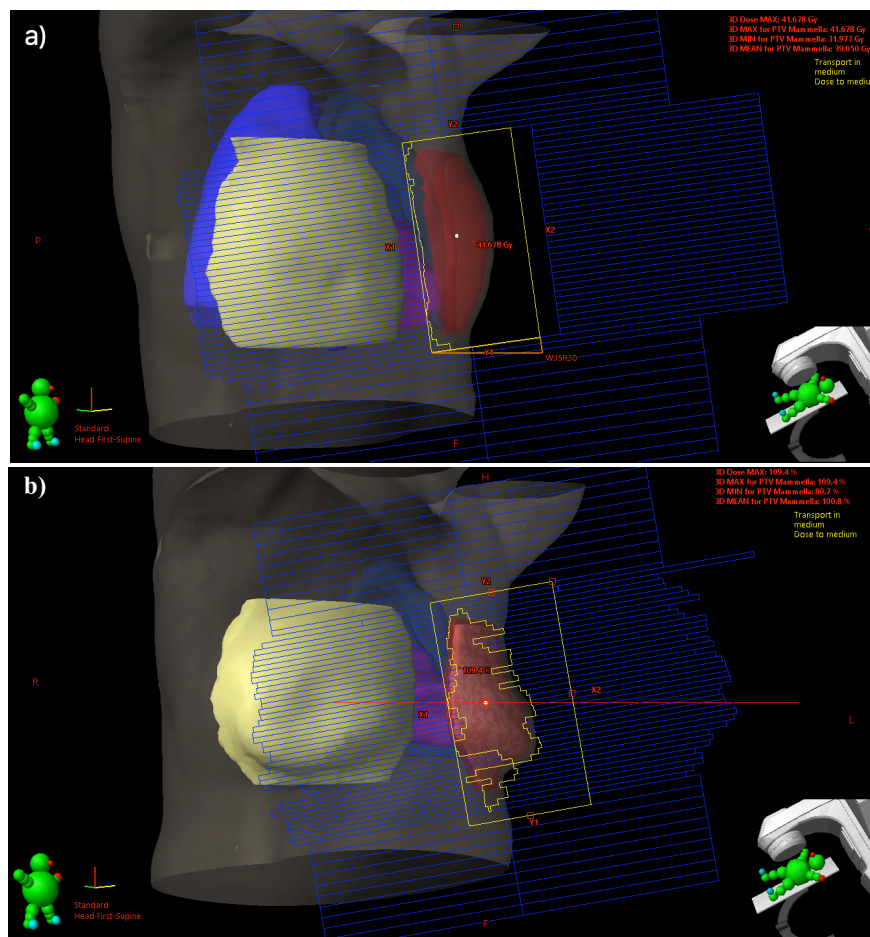


Figure 2.12: Screenshot of the TPS graphical interface in BEV view, the blue grid is the multileaf collimator, according to its position the field shape (yellow) varies. a) BEV view in 3D-CRT, b) VMAT irradiation.

Eclipse™ has been used to simulate all the measurements performed at HSR.

- Intercalibration of ionization chambers: a TPS simulate a PMMA phantom of $30 \times 30 \times 30 \text{ cm}^3$ irradiated with a uniform field of $10 \times 10 \text{ cm}^2$. To give 1 Gy of dose to water at the depth of 1.5 cm and 7.0 cm, it takes respectively 100 and 117 MU.
- EBT3 calibration: with the same phantom and field as before, at a depth of 1.5 cm, MU are calculated to achieve dose to water value in the range of 0.5 Gy to 9.0 Gy.
- WBI and PBI: To simulate a WBI, a TPS simulate a cylindrical PMMA phantom, with diameter $d = 14 \text{ cm}$ and height $h = 25 \text{ cm}$. A cylindrical target of $150 \times 20 \text{ mm}^2$ ($W \times H$) at the centre of the phantom is irradiated (at 360°) at 6 MV with a target dose of 6 Gy (Fig. 2.13). The source-to-axis is $SAD = 100 \text{ cm}$ and the calculated source-to-surface is $SSD = 97 \text{ cm}$. The TPS result is a value of UM of 899 MU to achieve the dose of 6 Gy to the target. To simulate a PBI, the TPS is the same, with the only difference in the cylindrical target dimension: $15 \times 20 \text{ mm}^2$ ($W \times H$) (Fig. 2.14). This time to achieve the dose of 6 Gy, 809 MU are necessary.

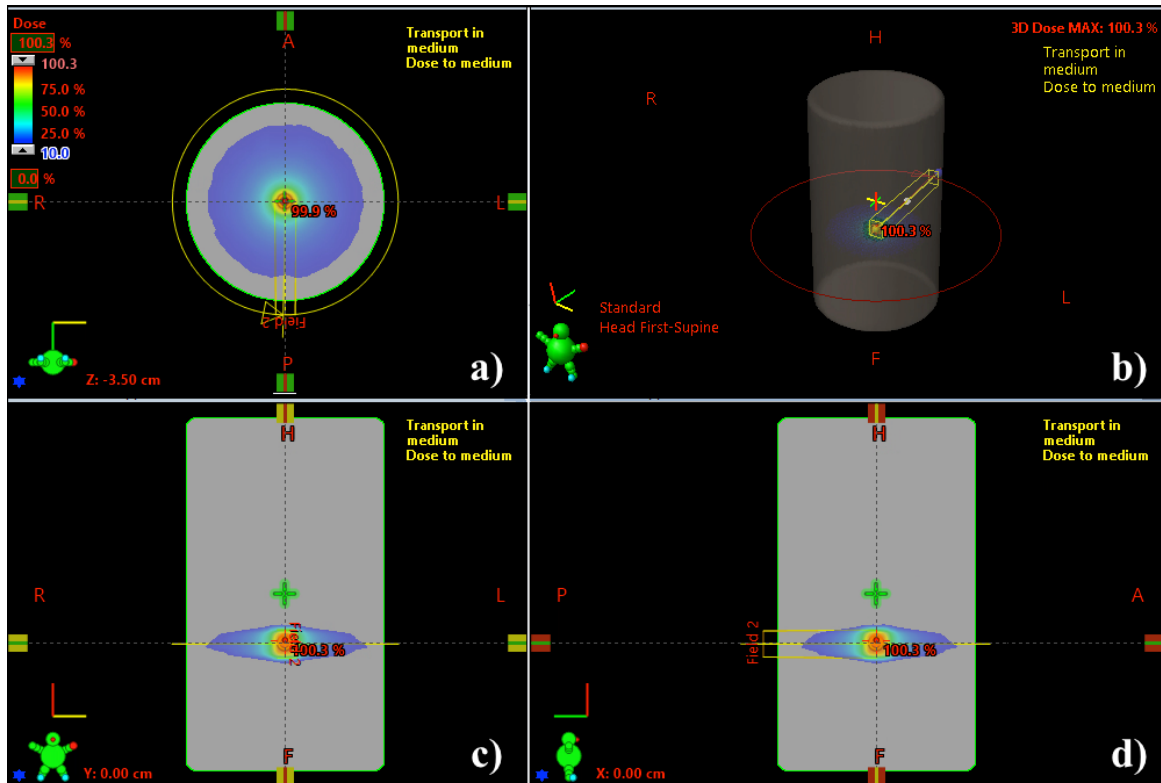


Figure 2.13: TPS simulation of the 14-cm diameter PMMA cylindrical phantom irradiated with a target dose of 6 Gy and with a beam size of $15 \times 20 \text{ mm}^2$. a) transversal view, b) BEV view, c) frontal view, d) sagittal view.

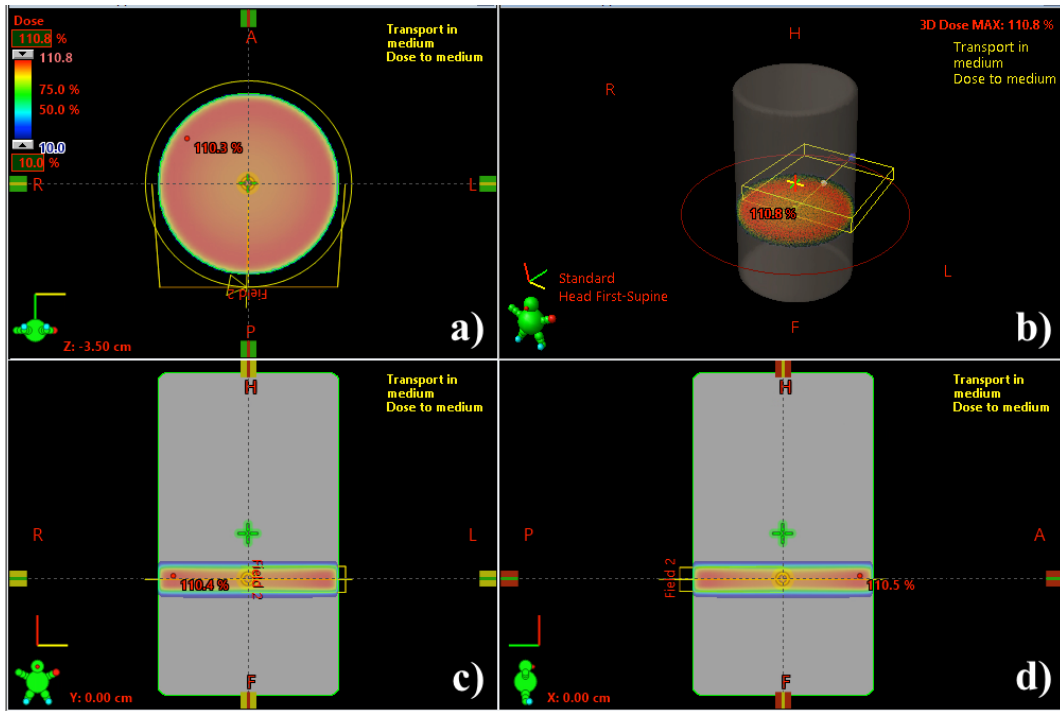


Figure 2.14: TPS simulation of the 14-cm diameter PMMA cylindrical phantom irradiated with a target dose of 6 Gy and with a beam size of $150 \times 20 \text{ mm}^2$. a) transversal view, b) BEV view, c) frontal view, d) sagittal view.

2.2.3 Measurements at San Raffaele Hospital

Measurements were performed at San Raffaele Hospital (HSR) on November 2017, using a Varian Clinac iX System Linac (Fig. 2.15). It is a high-energy accelerator with high intensity mode which permits to treat patients faster with the ability to deliver a high dose rate up to 2400 MU/min at 10 MV High-Intensity Mode. The Clinac system enables radiotherapy treatments in any area of the body. Clinac is highly versatile and enable a wide range of advanced features including IMRT, IGRT, VMAT, RapidArc and stereotactic radiosurgery [18]. *Eclipse™ treatment planning system* is the integrated software. In this work Clinac was used in RapidArc modality, which is a modality for volumetric treatments, able to deliver fast treatments using precise 3D dose distribution.

- Intercalibration of the ionization chambers

The dosimetry protocol followed the IAEA protocol, according to which: “It is assumed that the absorbed dose to water, D_w , is known at a depth of 5 g/cm^2 in a water phantom for ^{60}Co gamma rays. This is realized at the SSDL (Secondary Standard Dosimetry Laboratory) by means of a calibrated cavity ionization chamber performing measurements in a water phantom. The user chamber is placed with its reference point at a depth of 5 g/cm^2 in a water phantom and its calibration factor $N_{D,w}$ is obtained from:

$$N_{D,w} = D_w/M$$

where M is the dosimeter reading corrected for influence quantities, in order to correspond to the reference conditions for which the calibration factor is valid". Reference conditions recommended for the calibration of ionization chamber in ^{60}Co are reported in the IAEA protocol.



Figure 2.15: Varian Clinac iX System Linac [18]

Following the IAEA protocol, the hospital linear accelerator is calibrated with a Farmer® Ionization Chamber, type 30010 (PTW Freiburg, Germany) (Fig. 2.16a), in water at standard temperature and pressure, so that 100 Monitor Unit (MU) (which are the measurement units adopted for dose delivery at the Linac console) correspond to 1 Gy of D_w at 5-cm deep in water. In order to accommodate the ionization chamber in the cavity inside the phantom, we used a Semiflex Ionization Chamber, type 31010 (PTW Freiburg, Germany) (Fig. 2.16b). This implied the necessity to perform a dosimetric intercalibration between the two chambers (Farmer and Semiflex).

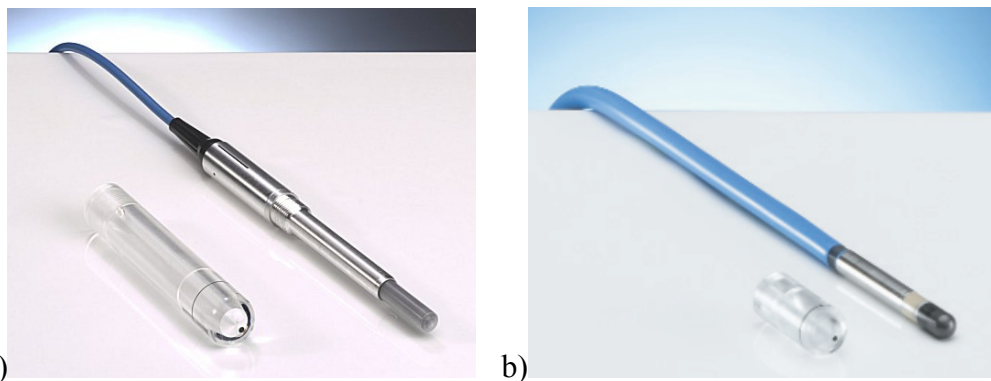


Figure 2.16: a) Farmer® Ionization Chamber, type 30010; b) Semiflex Ionization Chamber, type 31010.

At the time of the measurements, temperature and pressure values were respectively: $T = 20.5^{\circ}\text{C}$, $P = 1011 \text{ mbar}$ – measured with an Oregon Scientific meteo station. So the temperature and pressure correction factor, TCF, was:

$$TCF = \frac{(273.15 + T(^{\circ}\text{C}))}{(273.15 + T_0)} * \frac{P_0}{P (\text{mbar})} = 1.004 \quad (12)$$

where $P_0 = 101.3 \text{ kPa}$ and $T_0 = 20^{\circ}\text{C}$.

Both chambers were positioned on the patient bed of the Clinac iX System, sandwiched into PMMA slabs, with apposite holes to accommodate them. A first measurement was performed with the chambers under 1.5 cm of PMMA (build-up depth, at which there is the maximum of dose deposition), then the measurement was repeated under 7 cm of PMMA (a depth of 7 cm is chosen because in next measurements EBT-3 film were positioned in the central plane of the PMMA phantom, that is at 7 cm deep) (Figs. 2.17 and 2.18). They were in the centre of the irradiation field of $10 \times 10 \text{ cm}^2$, and were irradiated with a dose rate of 600 MU/min, so the corresponding dose to water was $D_w = 1 \text{ Gy}$. The irradiation was static and uniform. The MUs necessary for a target dose of 1 Gy were previously calculated with EclipseTM TPS. Measurements were performed at constant source-to-axis distance, SAD = 100 cm, so the source-to-surface distance (SSD) varies according to the depth of the chamber in the PMMA. For each irradiation, the corresponding charge value, C, was measured with a UNIDOS® E Universal Dosemeter (PTW Freiburg, Germany) connected to the ionization chambers. This value was then corrected for the TCF value as follows:

$$C^{\text{corr}} = C * TCF. \quad (13)$$

Results of the measurements are reported in table 2.2.

Table 2.2: For each chamber are reported the depth in the PMMA slabs, the corresponding SSD, the monitor units delivered, the measured charge, C, and the corrected charge, C^{corr} .

Chamber	d (cm)	SSD (cm)	MU	C (nC)	C^{corr} (nC)
Farmer	1.5	98.5	100	22.49 ± 0.01	22.57 ± 0.01
Farmer	7.0	93	117	22.97 ± 0.01	23.05 ± 0.01
Semiflex	1.5	98.5	100	3.410 ± 0.001	3.423 ± 0.001
Semiflex	7.0	93	117	3.463 ± 0.001	3.476 ± 0.001

Adopting the IAEA protocol TRS-398, 100 MU at 1.5 cm of depth in the PMMA correspond to 1 Gy of D_w . So, known the corrected charge at 1.5-cm of depth, $C_{1.5}^{\text{corr}}$, the unknown is the dose measured by the Semiflex at 7.0 cm of depth. With a simple proportion, using the

corrected charge calculated for the Semiflex at 1.5 cm of depth, the intercalibration factor, IF, is:

$$IF = \frac{1}{C_{1.5}^{corr}} = (0.29218 \pm 0.00008) \text{ Gy/nC} \quad (14)$$

In this way at 7 cm, 117 MU measured with the Semiflex correspond to a value of D_w equal to:

$$D_w = C_{7.0}^{corr} * FI = (1.015 \pm 0.015) \text{ Gy} \quad (15)$$

where the uncertainty on D_w is equal to 1.5%, as indicated in the IAEA protocol. In this way the dose measured by the Semiflex corresponds to the dose simulated by Eclipse™, the intercalibration factor will be important for the next measurements, because it allows to obtain the dose value from the charge value measured by the Semiflex.

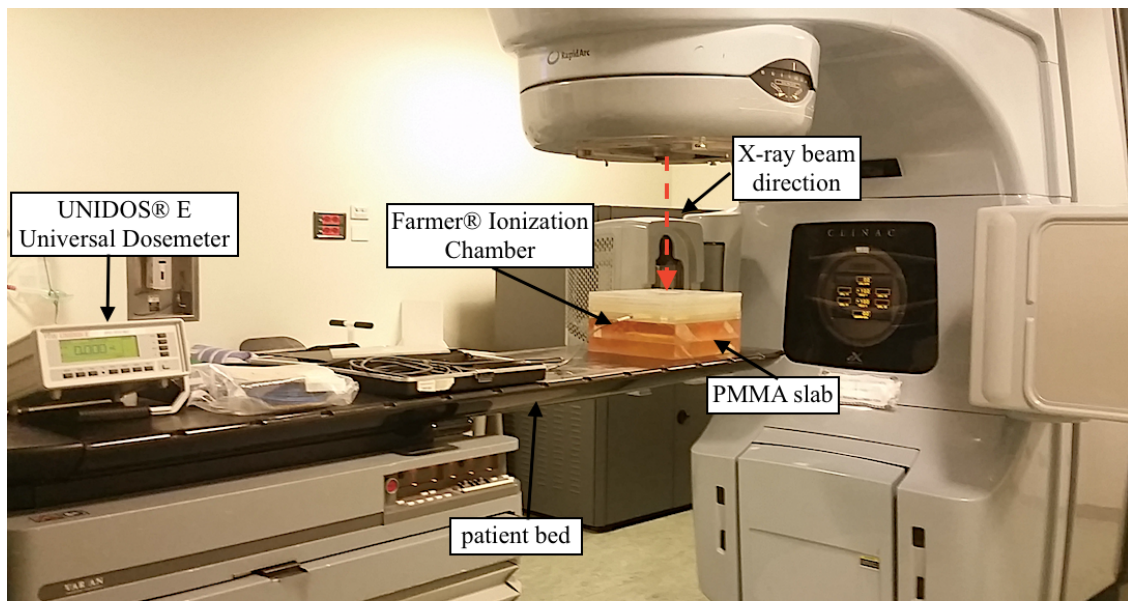


Figure 2.17: Photo of the experimental setup. On the left there is the UNIDOS® E Universal Dosimeter connected to the Farmer®; in the centre there is the Farmer® sandwiched in PMMA slabs; on the right there is the Varian Clinac iX System Linac.

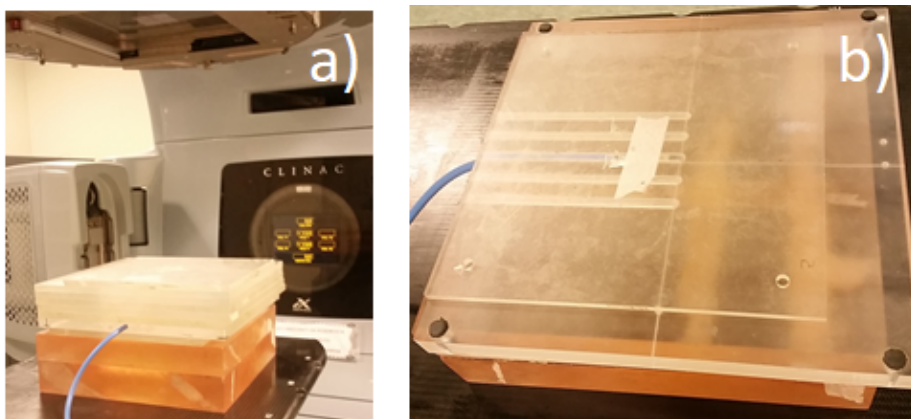


Figure 2.18: Photo of the experimental setup: the Semiflex is under 7 cm (a) and 1.5 cm (b) of PMMA slabs.

- **EBT3 calibration**

Dosimetric film calibration is done positioning EBT3 film pieces under 1.5-cm of a PMMA slab and irradiating them with different MU to deliver values of dose to water, D_w , in the range of 0.5 Gy – 9 Gy. Film pieces were cut in pieces of $3 \times 5 \text{ cm}^2$, positioned all in the same place of the PMMA phantom and in the centre of the irradiation field of $10 \times 10 \text{ cm}^2$ (Fig. 2.19). Irradiation was static and uniform. The dose rate was of 600 Mu/min and the SSD = 100 cm. One piece of film was not irradiated and reserved as control. Following the protocol explained in paragraph 2.1.1, the average optical density change, $\overline{\Delta_{\text{netOD}}}$, and the corresponding standard deviation, $\sigma_{\overline{\Delta_{\text{netOD}}}}$, are calculated and reported in Table 2.3.

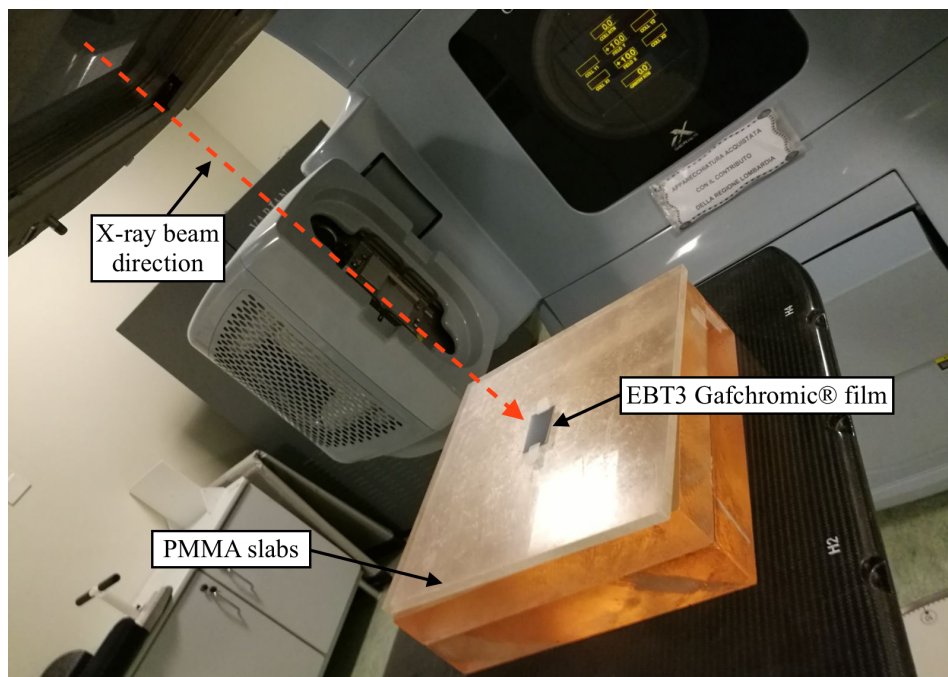


Figure 2.19: One piece of EBT3 is positioned in the centre of the PMMA slab.

Table 2.3: For each MU, there are the corresponding film name, dose to water value, D_w , and the average optical density change.

MU	# film	D_w (Gy)	$\overline{\Delta_{\text{netOD}}} \pm \sigma_{\overline{\Delta_{\text{netOD}}}}$
50	B07	0.500 ± 0.007	0.05303 ± 0.00012
100	B02	1.000 ± 0.015	0.0976 ± 0.0002
120	B04	1.20 ± 0.02	0.1136 ± 0.0003
180	B05	1.80 ± 0.03	0.1574 ± 0.0004
200	B01	2.00 ± 0.03	0.1705 ± 0.0004
300	B09	3.00 ± 0.04	0.2328 ± 0.0006
500	B06	5.00 ± 0.07	0.3315 ± 0.0009
700	B03	7.00 ± 0.10	0.4078 ± 0.0011
900	B10	9.00 ± 0.13	0.4660 ± 0.0012

Values in Table 2.3, are used to evaluate the calibration curve. The more suitable fitting function is the power function: $y = a*x + b*x^n$ (Fig. 2.20).

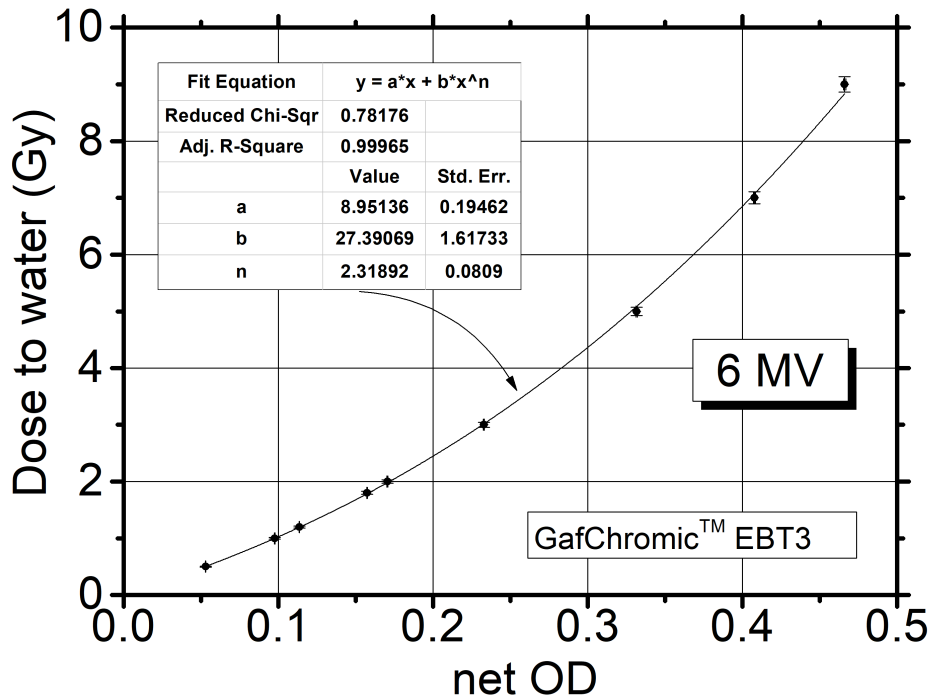


Figure 2.20: Calibration curve for the EBT3 film at 6 MV.

- PBI and WBI of the phantom

Measurements were performed using a 14-cm diameter PMMA cylindrical phantom (the same phantom of paragraph 2.1.2), simulating a pendant breast. The purpose of the measurements is to evaluate the two-dimensional (2D) dose map in a whole breast irradiation (WBI) and in a partial breast irradiation (PBI). To realize them, we plan to irradiate a cylindrical target of different dimensions at the centre of the phantom:

- in the WBI the target size was $150 \times 20 \text{ mm}^2$ (W \times H);
- in the PBI the target size was $15 \times 20 \text{ mm}^2$ (W \times H).

Measurements were performed using a Varian Clinac iX System Linac, with the beam rotating all around the phantom in order to have a target dose of 6 Gy in the centre of the phantom. The PMMA phantom was positioned horizontally along the patient bed, with the axis of rotation of the beam coincident with the axis of rotation of the phantom. The alignment of the phantom was done with the field lights and positioning lasers, and by moving the robotized bed appropriately. As the alignment was done almost in the dark, to be sure of the exact position of the Semiflex sensitive volume and the centre of target to be irradiated, scotch tape was used to marks these two reference points (Fig. 2.21).

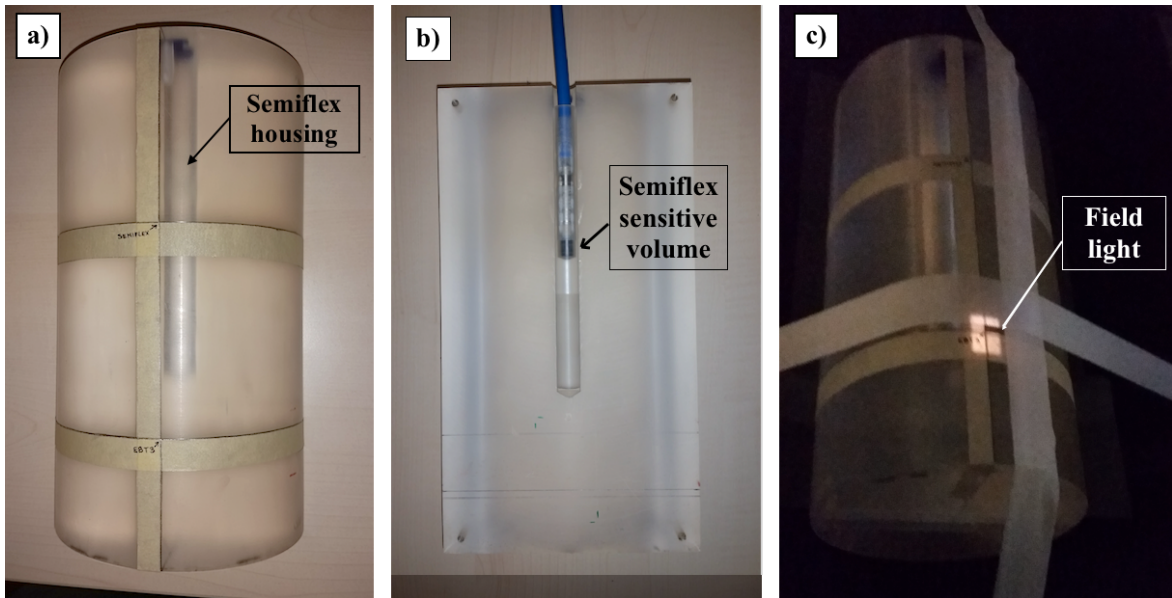


Figure 2.21: Photos of the 14-diameter PMMA cylindrical phantom. Scotch tape marks two reference points (a): the centre of the Semiflex sensitive volume (b) and the centre of the target to be irradiate. (c) Field light allows see the irradiated area of size $1.5 \times 2.0 \text{ cm}^2$ ($H \times W$).

Measurements were performed at temperature and pressure of: $T = 20.5^\circ\text{C}$ and $P = 1011$ mbar, so the temperature and pressure correction factor, TCF, according to the (12), was:

$$\text{TCF} = 1.004$$

The source to surface distance was $\text{SSD} = 93$ cm. Before starting the measurements, both configurations were simulated with EclipseTM TPS. For a target dose of 6 Gy in the centre of the phantom with a dose rate of 600 MU/min, 809 MU are necessary in WBI, while 899 MU are necessary in PBI.

The Semiflex chamber was positioned in the phantom housing, at 7 cm depth, and irradiated in the same conditions as explained for WBI and PBI, in order to compare its measured dose, D , with the dose evaluated by Eclipse TPS, D_{TPS} . Charge measured by the ionization chamber was read for the dosimeter, corrected for the TCF and converted in dose using the intercalibration factor, IF. Results as reported in table 2.4, and C and C^{corr} are comparable within the experimental error.

Table 2.4: Comparison between the simulated dose by EclipseTM, D_{TPS} , and the measured dose by the Semiflex, D_s . MU, measured charge, C , and corrected charge, C^{corr} , are also reported for both WBI and PBI measurements.

	MU	D_{TPS} (Gy)	C (nC)	C^{corr} (nC)	D_s (Gy)
WBI	809	6	20.16 ± 0.01	20.23 ± 0.01	5.91 ± 0.09
PBI	899	6	20.27 ± 0.01	20.34 ± 0.01	5.94 ± 0.09

In order to evaluate the dose distribution, three calibrated EBT3 radiochromic films were inserted at the mid-plane in the phantom (Fig. 2.22). The first irradiation was with an X-ray beam of $150 \times 20 \text{ mm}^2$ ($W \times H$) for the WBI, the second was of $15 \times 20 \text{ mm}^2$ ($W \times H$) for the PBI. The 2D dose maps were acquired after a complete rotation of the beam around the phantom. Figure 2.23 shows the EBT3 radiochromic films after being irradiated.



Figure 2.22: a) Photo of the experimental setup, the 14-cm diameter PMMA cylindrical phantom is on the patient bed stopped with scotch tape (first plane) and the Clinac irradiate a cylindrical volume with the beam size of $1.5 \times 2.0 \text{ cm}^2$ (background). b) 14-cm diameter PMMA cylindrical phantom with three EBT3 film inserted in the mid-plane.

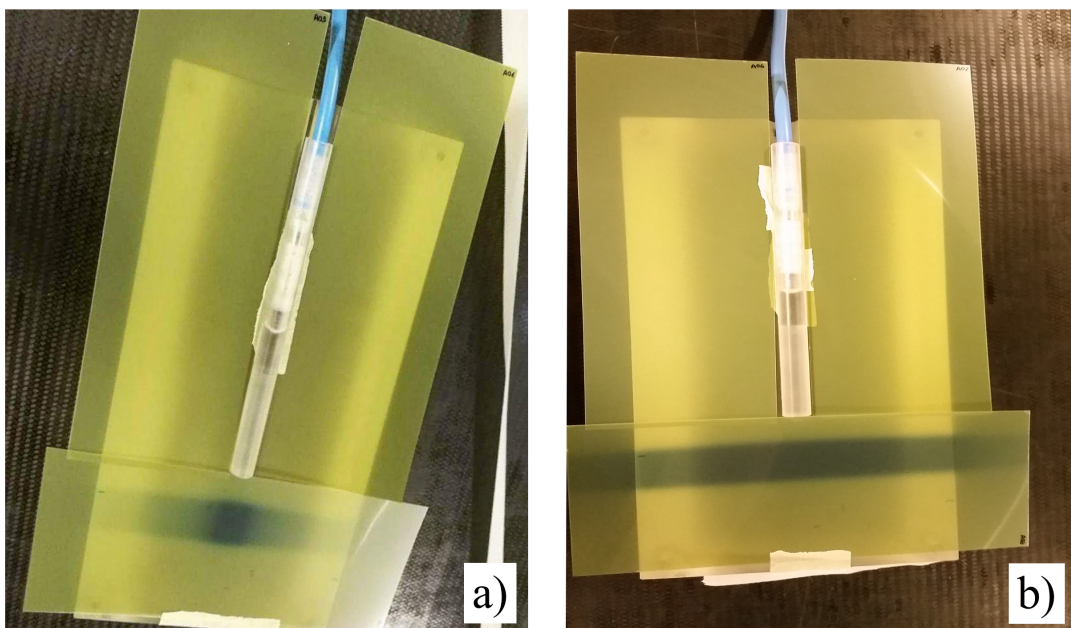


Figure 2.23: Photo of EBT3 radiochromic films inserted in the mid-plane of a 14-cm diameter PMMA cylindrical phantom after being exposed to a PBI (a) and to a WBI (b). A Semiflex ionization chamber is positioned in the phantom housing.

The images of each film were suitably assembled to create the 2D dose maps at mid-plane in the PMMA phantom.

Regarding the WBI measurements at 6 MV, Fig. 2.24 shows the 2D dose map (Fig. 2.24a), the isodose lines (Fig. 2.24c) and the horizontal profile evaluated along the centre of the irradiated area (Fig. 2.24b). The horizontal profile (Fig. 2.24b), corresponding to the radial dose profile, is cup-shaped in the central part with a minimum dose of about 6 Gy along the central axis of the cylindrical phantom and a maximum of about 6.5 Gy at 1.5 cm of depth in the PMMA phantom due to the build-up effect.

Figure 2.25 shows in detail the isodose curves in the range of 0.1 Gy to 6 Gy. A 3D representation of this dose distribution is shown in figure 2.26.

Figure 2.27 represents the isodose curves at the mid-plane of the phantom obtained with Eclipse™ software. The distance of 1.66 cm represents the distance of the isodose curve of the 5% from the centre of irradiation. While the distance of measured isodose curve of 5% is of 1.9 cm. This result is acceptable when considering that the simulation software of the TPS does not take perfectly into account the physical phenomena of the scattered radiation which will contribute to an increased dose at a distance from the target.

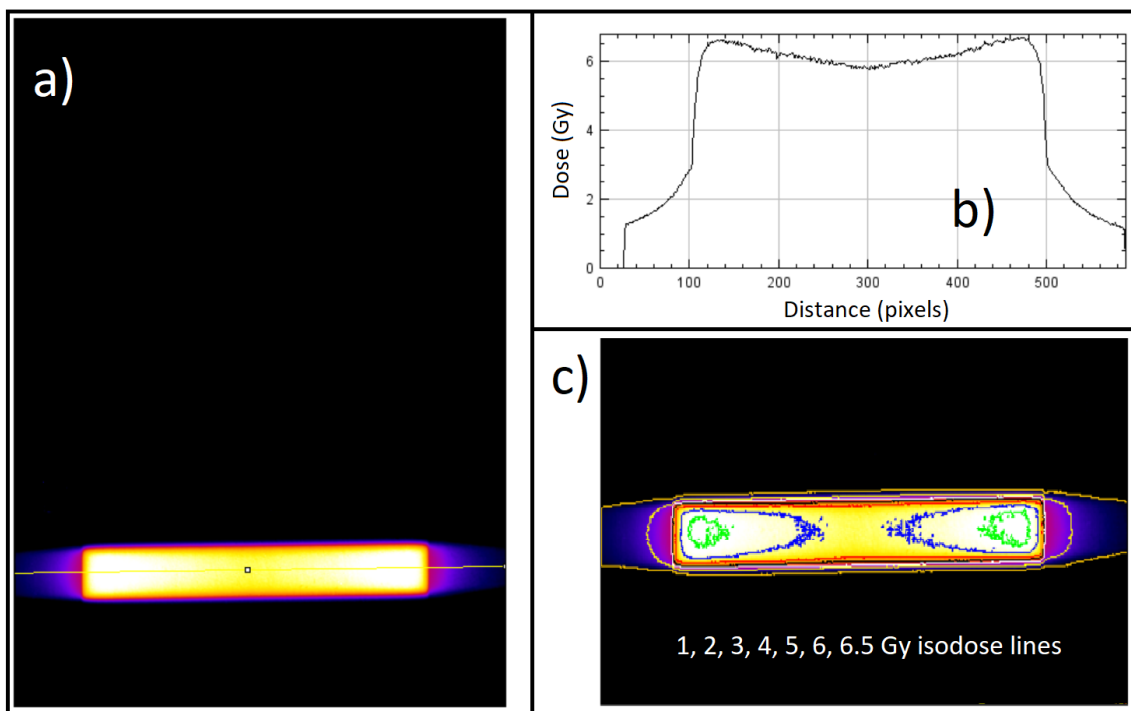


Figure 2.24: a) 2D dose map at the mid-plane in the 14-cm diameter PMMA phantom obtained in WBI, the pixel values are in dose to water in Gy. b) Horizontal dose profile along the yellow line depicted in a) gives a cupped profile. c) Isodose curves of the 2D dose map.

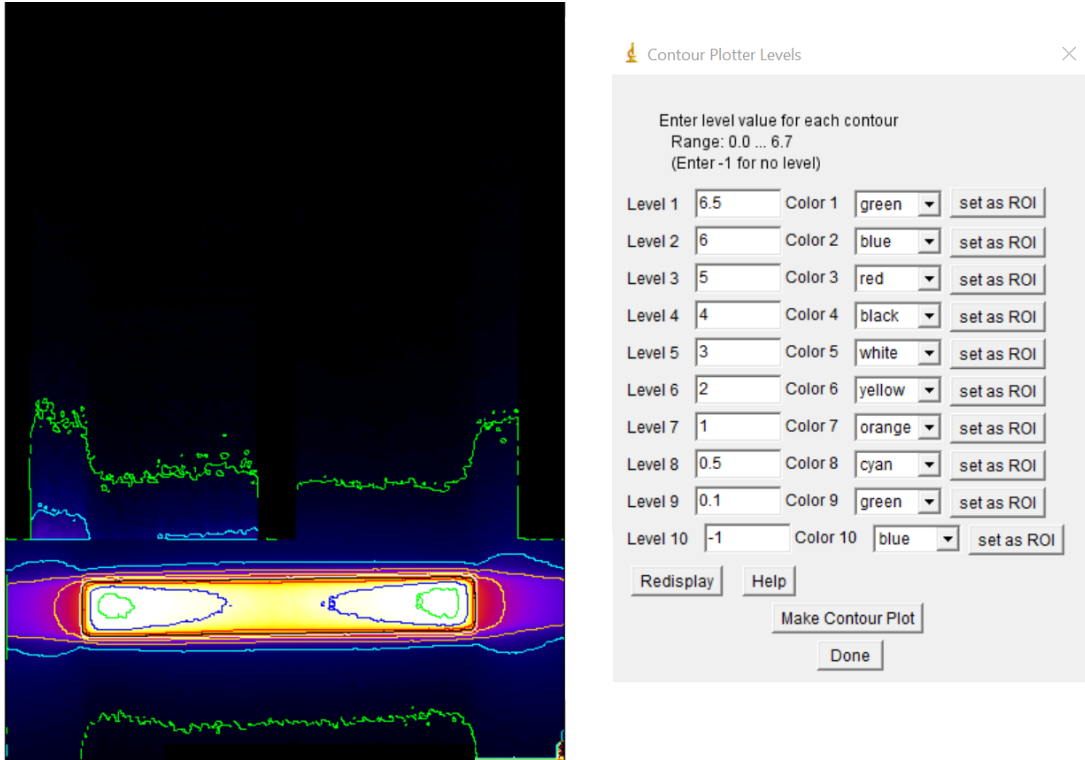


Figure 2.25: Isodose curves at the mid-plane in the 14-cm diameter PMMA phantom obtained in WBI. The pixel value were normalized to the maximum. The isodose legends in percent of the maximum dose are indicated on the subpanel on the right side.

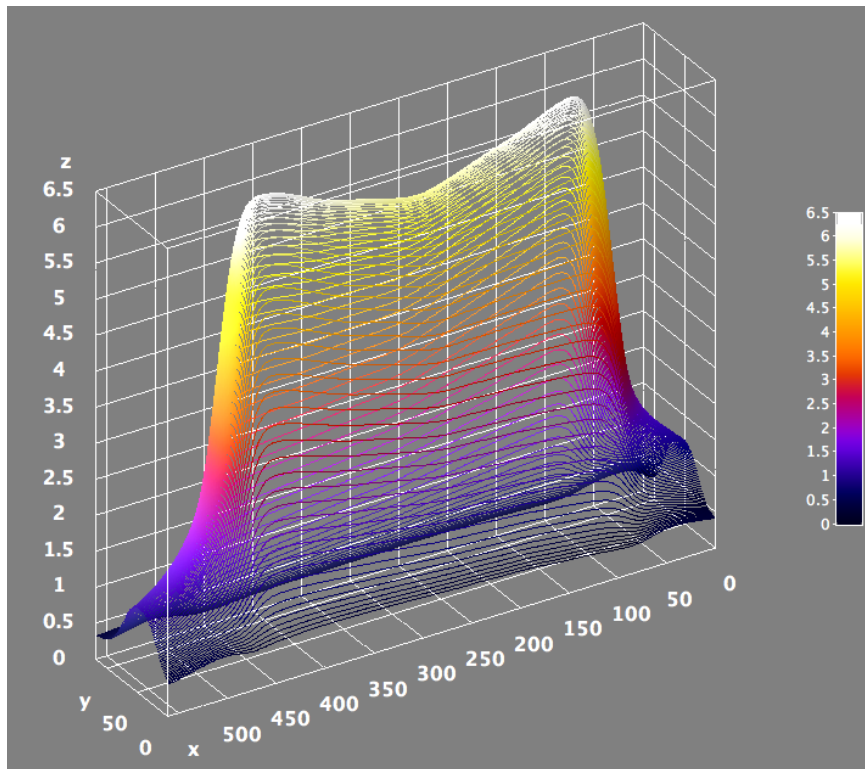


Figure 2.26: 3D dose map corresponding to data shown in figure 2.24. The two peaks reflect the maximum of depth of dose deposition below the surface of the phantom, due to the build-up effect of the 6 MV rotational irradiation of the cylindrical PMMA phantom.

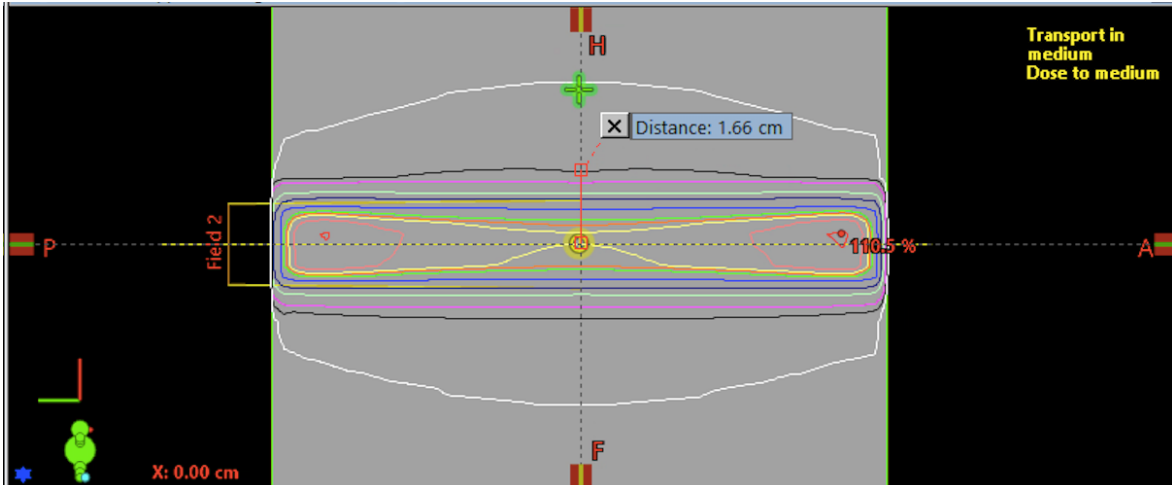


Figure 2.27: Isodose curves at the mid-plane in the 14-cm diameter PMMA phantom obtained in WBI simulation with Eclipse™ software. The distance of 1.66 cm represents the distance of the isodose curve of the 5% from the centre of irradiation.

Regarding the PBI measurement at 6 MV, figure 2.28 shows the 2D dose map (Fig. 2.28a), the isodose lines (Fig. 2.28c) and the horizontal profile evaluated along the centre of the irradiated area (Fig. 2.28b). The principle of dose summation along the axis of rotation produced a dose distribution peaked at the centre of rotation, with a peak width of 1.5 cm at 85% of the maximum dose. Figure 2.29 shows the isodose curves in the range of 0.1 Gy to 6 Gy. A 3D representation of dose distribution is shown in figure 2.30. Figure 2.31 shows the line profiles along the vertical direction evaluated at 1 cm (ROI 1 of fig. 2.28) and at 5 cm (ROI 2 of fig. 2.28) from the cylinder axis. Both profiles were normalized to the maximum value (6 Gy) of the 2D dose map of figure 2.28. The profile at 1 cm from the cylindrical axis has a peak value of 55% of the target dose, while at 5 cm the peak value is 11% of the target dose. When considering the dose attained at a distance from the target dose in the direction of the chest wall (i.e. from bottom to top in fig. 2.28), we found that the dose at 5 cm from the target was less than 0.01% of the target dose in ROI 1, and less than 0.0001% of the target dose in ROI 2.

Figure 2.31 represents the isodose curves at the mid-plane of the phantom obtained with Eclipse™ software. The distance of 1.42 cm represents the distance of the isodose curve of the 5% from the centre of irradiation. While the distance of measured isodose curve of 5% is of 1.7 cm, in analogy with the WBI measurement.

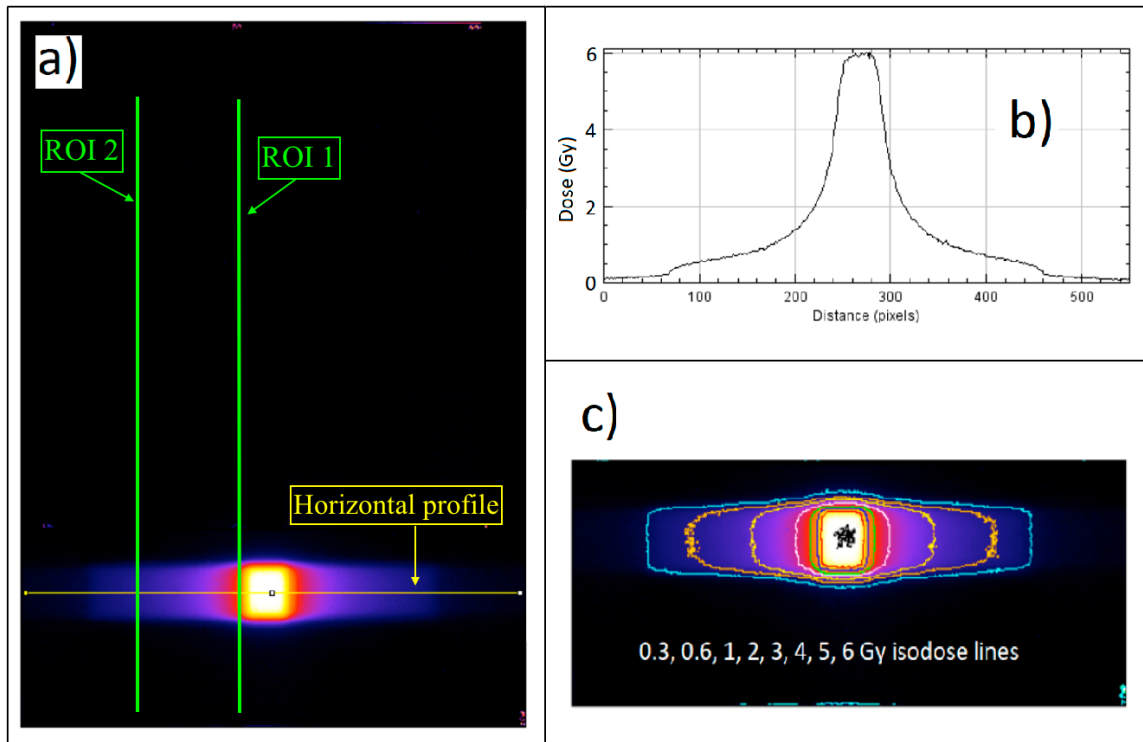


Figure 2.28: a) 2D dose map at the mid-plane in the 14-cm diameter PMMA phantom obtained in PBI, the pixel values are in dose to water in Gy. b) Horizontal dose profile along the yellow line depicted in a) gives a profile peaked in the centre. c) Isodose curves of the 2D dose map.

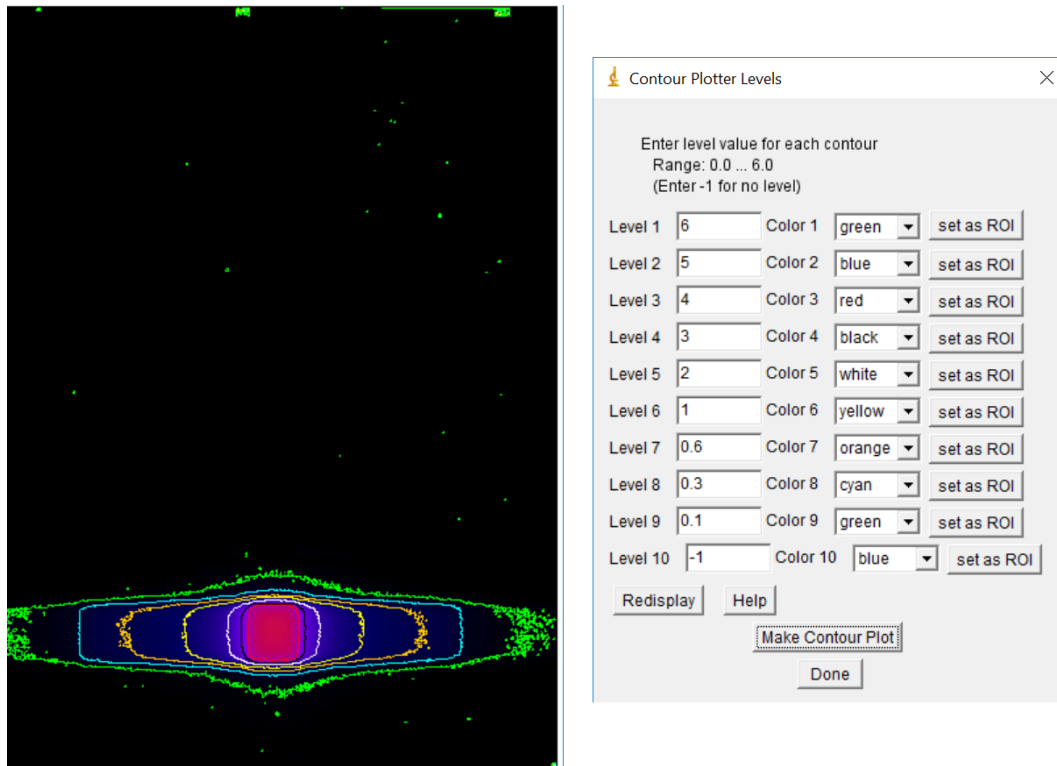


Figure 2.29: Isodose curves at the mid-plane in the 14-cm diameter PMMA phantom obtained in PBI. The pixel value were normalized to the maximum. The isodose legends in percent of the maximum dose are indicated on the subpanel on the right side.

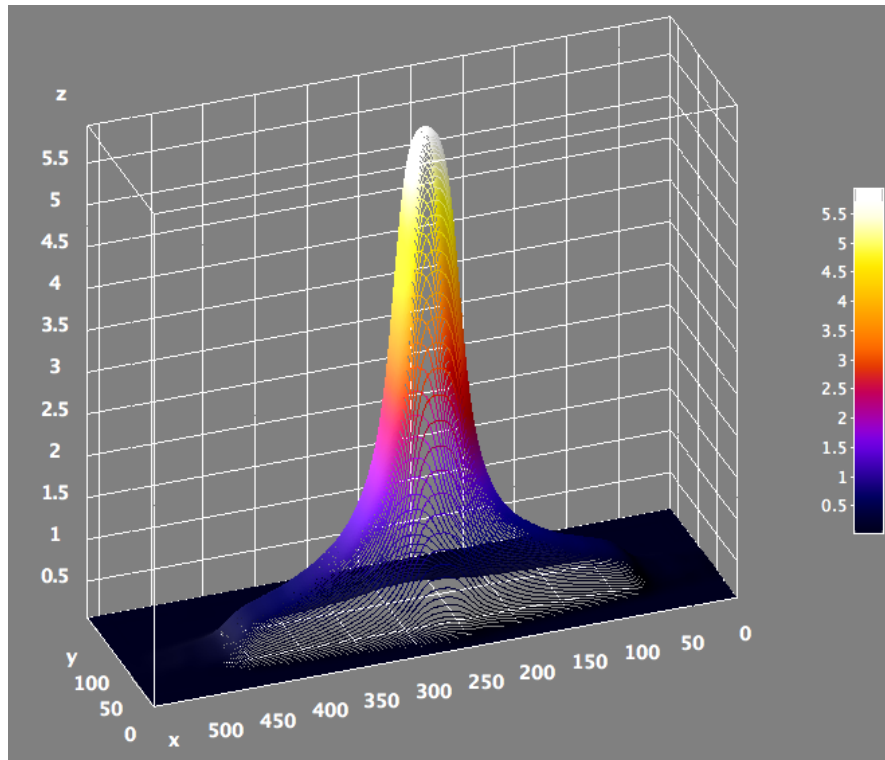


Figure 2.30: 3D dose map corresponding to data shown in figure 2.27. The central peak is due to the principle of dose summation along the axis of rotation at 6 MV in rotational irradiation of the cylindrical PMMA phantom.

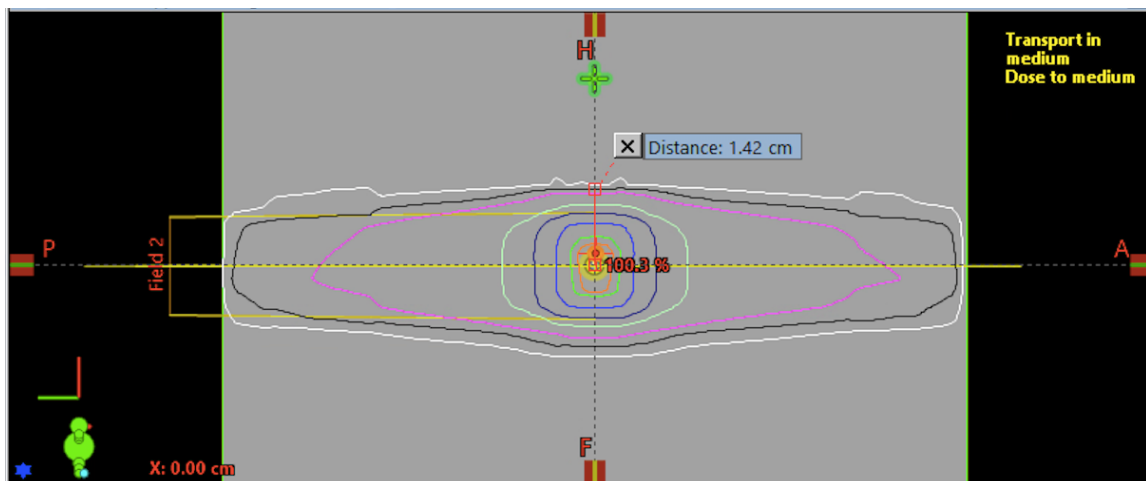


Figure 2.31: Isodose curves at the mid-plane in the 14-cm diameter PMMA phantom obtained in PBI simulation with Eclipse™ software. The distance of 1.42 cm represents the distance of the isodose curve of the 5% from the centre of irradiation.

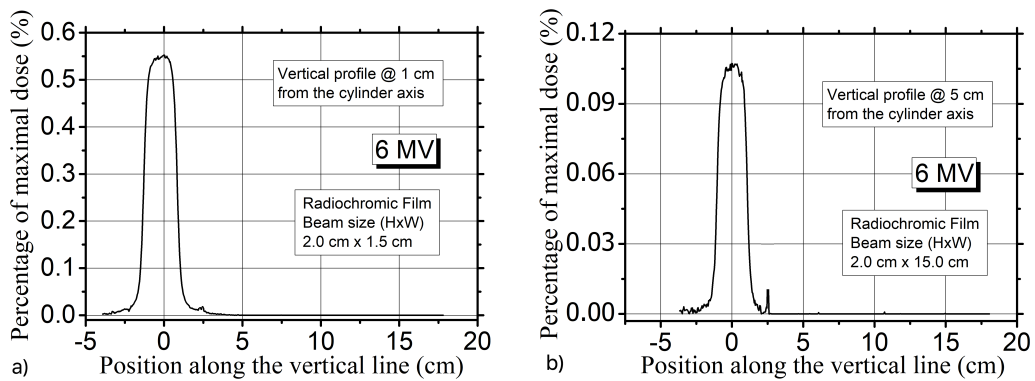


Figure 2.32: Vertical average profile evaluated in the radiochromic film dose map at 1 cm (a) and 5 cm (b) from the cylinder axis at 6 MV.

In order to evaluate the background, a vertical profile in a ROI far from the centre of irradiation was considered (fig. 2.33). As a result, the background is the less than 5% of the target dose (6 Gy).

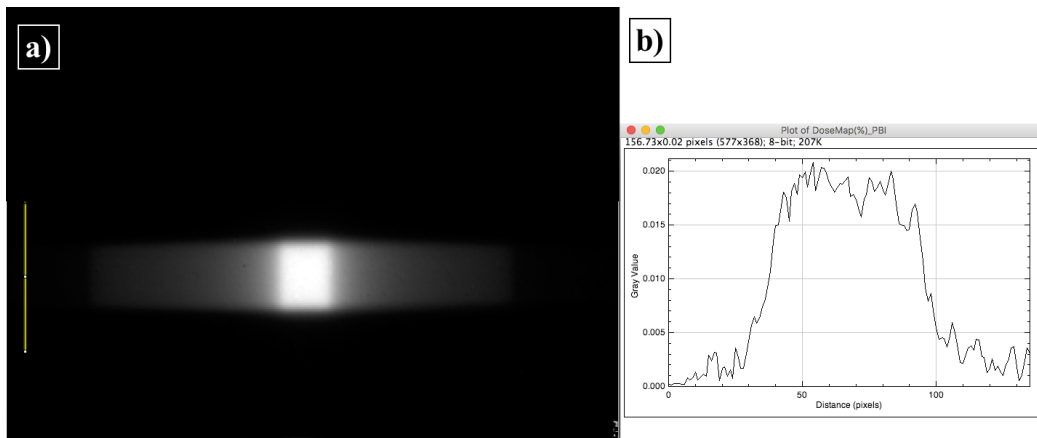


Figure 2.33: b) Vertical profile on a the 2D dose map of PBI measurement (a).

In order to compare WBI and PBI measurement, the radial dose profiles in both measurements were evaluated along the horizontal profile from the central point of the irradiation toward the periphery, and reported in fig. 2.34. For the beam with of 15 cm a cupped profile is observed, while for 1.5-cm collimation a dose distribution peaked in the centre is found. Please remember that the phantom radius is of 7 cm, so dose values farther then 7 cm from the phantom axis are recorded from film pieces that come out from the phantom and are free in air. Periphery-to-centre dose ratio is evaluated at 6.5 cm and ranges between 8.0% for PBI and 100% for WBI. To evaluates the skin-sparing factor, the dose at 7 cm from the centre was divided by the dose to the centre. This results in a 6% of the target dose to the skin for PBI and 96% for WBI, so only PBI ensures the skin sparing.

Differences in dose distribution for the irradiation of a localized target between 100 keV and 6 MV are collected in table 2.5 for PBI measurements and in table 2.6 for WBI measurements.

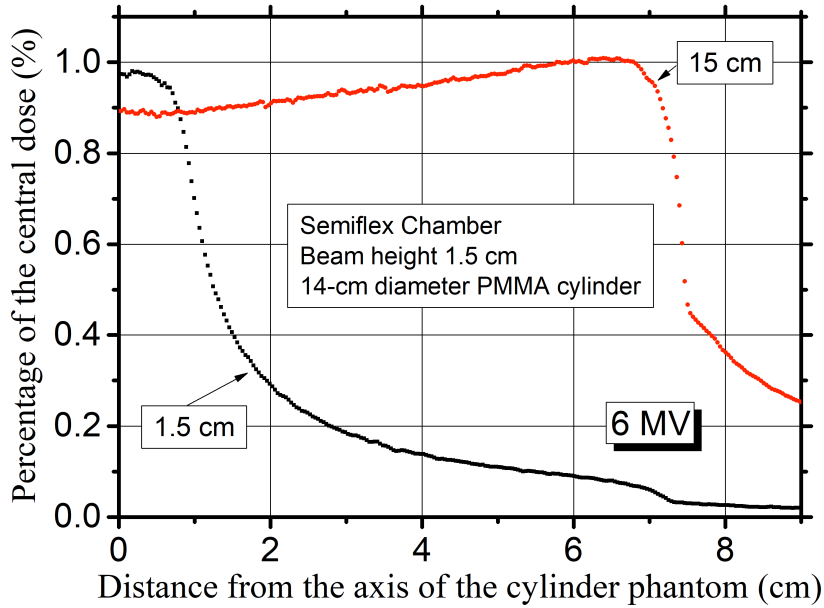


Figure 2.34: Percentage of the central dose in a 14-cm diameter PMMA cylindrical phantom for beam width of 1.5 and 15 cm at 6 MV.

Table 2.5: Result of PBI measurement, beam collimation was 1.5 cm in both cases. Results in percentage are compared to the target dose. The hundred percent dose correspond to 7 Gy for 100 keV and 6 Gy for 6 MV. The corresponding uncertainties are 0.1 Gy and 0.09 Gy, respectively.

	100 kV with SR	6 MV with VMAT
Horizontal profile shape	Distribution peaked in the centre. Peak width is 1.5 cm at 85% of the maximum dose.	Distribution peaked in the centre. Peak width is 1.5 cm at 85% of the maximum dose.
Percentage of dose at 1 cm	100%	55%
Percentage of dose at 5 cm	23%	11%
Periphery-to-centre dose ratio (at 6.5 cm)	12%	8%
Skin-sparing ratio (at 7 cm)	15%	6%
Vertical profile at 5 cm from the peak at 1 cm from the centre	5%	> 0.01%
Vertical profile at 5 cm from the peak at 5 cm from the centre	1%	> 0.0001%

Table 2.6 Result of WBI measurements, beam collimation was 16 cm at 100 keV with SR, and 15 cm at 6 MV with VMAT. Results in percentage are compared to the target dose. The hundred percent dose correspond to 7 Gy for 100 keV and 6 Gy for 6 MV. The corresponding uncertainties are 0.1 Gy and 0.09 Gy, respectively.

	100 kV with SR	6 MV with VMAT
Horizontal profile shape	Cupped profile in the central part with a minimum in the centre and a maximum on the surface of the phantom.	Cupped profile in the central part with a minimum dose along the central axis and a maximum at 1.5 cm of depth in the phantom due to the build-up effect.
Periphery-to-centre dose ratio (at 6.5 cm)	156%	100%

The uncertainty on the dose values is of 1.5% for all measurements.

At 6 MV with VMAT in the SR³T geometry (pendant breast) the dose is more conformed compared to 100 keV with SR in the same geometry. VMAT confirms to be able to provide a highly conformant dose to the target, and the full circle rotation allows to determine a symmetrical dose distribution with less than 1% of the dose at the skin surface.

Conclusions

This thesis work is born in the development of a new technique of radiotherapy of breast cancer using a high intensity monoenergetic SR beam: the synchrotron radiation rotational radiotherapy (SR³T), and analyses the differences in dose distribution for the irradiation of a localized target between 100 keV and 6 MV.

This thesis provided experimental evidence of the comparable dose distributions obtained in simulated whole breast and partial breast irradiation with 100 keV and 6 MV beams. The megavoltage irradiation (VMAT with an arc of 360 degrees) provide additional skin sparing by the build-up effect, but the full circle rotation cannot be adopted for prone or supine position of the patient since the accelerated gantry can rotate only around an horizontal axis. In SR³T the beam is fixed and it is the patient bed that rotates around a vertical axis with the patient in prone position. At 100 keV irradiation the dose toward the chest wall at 7 cm from the target volume is 15% of the target dose: for comparison, in the protocol for whole breast irradiation at San Raffaele Hospital, the mean dose to the breast should not exceeds the 12% of the target dose.

Overall the results here provided confirm the feasibility of kilovoltage rotational radiotherapy of breast cancer; further work will be dedicated to the specific task of partial breast irradiation which appears to offer the highest interest for small tumours, of the size (a few cm³) investigated in the present thesis.

Bibliography

- [1] www.airc.it
- [2] Khan F. M., Gibbons. J. P. *The physics of radiation therapy*. Lippincott Williams & Wilkins. 5th ed. (2014)
- [3] Di Lillo F., *Breast cancer: imaging and radiotherapy with synchrotron radiation*. PhD thesis, University of Naples Federico II, Naples, November 2017.
- [4] Darby S.C., Ewertz M., McGale P., Bennet A.M., Blom-Goldman U., Brønnum D., Correa C., Cutter D., Gagliardi G., Gifante B., Jensen M.B., Nisbet A., Peto R., Rahimi K., Taylor C., Hall P., *Risk of ischemic heart disease in women after radiotherapy for breast cancer*. N. Engl. Med. (2013); **368**, 987–998.
- [5] Mast M.E., Vredeveld E.J., Credoe H. M., van Egmond J., Heijenbrok M.W., Hug E.B., Kalk P., van Kempen-Harteveld L.M.L., Korevaar E.W., van der Laan H.P., Langendijk J.A., Rozema H.J.E., Petoukhova A.L., Schippers J.M., Struikmans H. and & Maduro J. H., *Whole breast proton irradiation for maximal reduction of heart dose in breast cancer patients*. Breast Cancer Res. Treat. (2014); **148**(1), 33–39.
- [6] Rahimi R., Timmerman R., *New technique for irradiating early stage breast cancer: stereotactic partial breast irradiation*. Seminars in Radiation Oncology (2017); Vol. **27**, issue 2, 279-288.
- [7] Pogdorsak E.B., *Radiation oncology physics: a handbook for teachers and students*. (2005); ISBN 92-0-107304-6
- [8] Cozzi L., Lohr F., Fogliata A., Franceschini D., De Rose F., Filippi A.R., Guidi G., Vanoni V., and Scorsetti M., *Critical appraisal of the role of volumetric modulated arc therapy in the radiation therapy management of breast cancer*. Radiat Oncol (2017) **12**:200. DOI 10.1186/s13014-017-0935-4.
- [9] Bondiau P., Bahadoran P., Lallement M., *Robotic stereotactic radiation concomitant with neo-adjuvant chemotherapy for breast tumors*. Int J Radiat Oncol Biol Phys (2009) **75**(4):1041-1041.
- [10] Vermeulen S., Cotrutz C., Morris A., *Accelerated partial breast irradiation: Using the cyberknife as the radiation delivery platform in the treatment of early breast cancer*. Front Oncol **1**(43), (2011), <http://dx.doi.org/10.3389/fonc.2011.0043>

- [11] Vermeulen S., Haas J.A., *Cyberknife stereotactic body radiotherapy and cyberknife accelerated partial breast irradiation for the treatment of early breast cancer*. *Transl Cancer Res* 3(4):295-302, (2011), <http://dx.doi.org/10.3978/j.issn.2218-676X.2014.07.06>
- [12] Prionas N.D., McKenney S.E., Stern R.L. and Boone J.M. *Kilovoltage rotational external beam radiotherapy on a breast computed tomography platform: a feasibility study*. *Int. J. Rad. Oncol. Biol. Phys.* (2012) **84**(2), 533–539.
- [13] Sarno, A., Mettivier, G., Russo, P. *Dedicated breast computed tomography: basic aspects*. *Med. Phys.* (2015) **42**(6), 2786–2804.
- [14] De Lucia P.A., Mettivier G., Di Lillo F., Sarno A., and Russo P. *SR-EBRT: Synchrotron radiation external beam rotational radiotherapy for breast cancer treatment*. *Phys. Med., Suppl.* (2016), **32**, 19.
- [15] Di Lillo F., Mettivier G., Sarno A., Castriconi R., and Russo, P. *Towards breast cancer rotational radiotherapy with synchrotron radiation*. *Phys. Med.* (2017a) **41**, 20–25.
- [16] Devic S., Tomic N. and Lewis D., *Reference radiochromic film dosimetry: review of technical aspects*. *Phys. Medica* (2016) **32**(4), 541–556.
- [17] <https://www.varian.com/oncology/products/software/treatment-planning/eclipse-treatment-planning-system>
- [18] <https://www.varian.com/oncology/products/treatment-delivery/clinac-ix-system>

Acknowledgements

Innanzitutto vorrei ringraziare il mio relatore, il professore Paolo Russo, non solo per questo lavoro di tesi ma per tutto il supporto, la disponibilità e l'affetto che mi ha mostrato in questo mio percorso, per aver sempre creduto in me anche quando io stessa dubitavo, e soprattutto per avermi fatto ritrovare il piacere di fare le cose “per sfizio”.

Vorrei poi ringraziare il professore Giovanni Mettivier, la dott. Francesca Di Lillo e il dott. Antonio Sarno, per me pilastri del laboratorio di fisica medica, per la pazienza, per l'aiuto costante e soprattutto per le risate.

Grazie al mio correlatore, il professore Vincenzo Roca, per la sua bontà e per avermi consigliato durante questo lavoro di tesi.

Il lavoro sperimentale di questa tesi è stato possibile grazie al supporto dell'Ospedale San Raffaele di Milano, Italia, ed in particolare grazie al gruppo di radioterapia che mi ha concesso di effettuare misure all'acceleratore medicale. È stato molto gratificante ed istruttivo per me lavorare con il gruppo di fisica medica, da cui ho ricevuto un caloroso benvenuto e tanto sostegno in un'atmosfera amichevole. In particolare vorrei ringraziare: il dott. R. Calandrino, il dott. M. Cattaneo, il dott. C. Fiorino, la dott.ssa L. Perna, la dott. R. Castriconi e gli specializzandi di fisica medica che in quei giorni mi hanno dedicato il loro tempo.